IMMUNOLOGY

Pseudokinase STK40 promotes T_H1 and T_H17 cell differentiation by targeting FOXO transcription factors

Yuexiao Tao[1], Zhenyan Jiang[1], Huizi Wang[1], Jia Li[1], Xin Li[1], Jun Ni[1], Jiamin Liu[1], Hongrui Xiang[1], Chenyang Guan[1], Wei Cao[1], Dongyang Li[1], Ke He[2], Lina Wang[2], Jing Hu[2], Ying Jin[2,3], Bing Liao[2]*, Ting Zhang[4]*, Xuefeng Wu[1]*

Inappropriate $CD4^+$ T helper (T_H) cell differentiation leads to progression of inflammatory and autoimmune diseases, yet the regulatory mechanisms governing stability and activity of transcription factors controlling T_H cell differentiation remain elusive. Here, we describe how pseudokinase serine threonine kinase 40 (STK40) facilitates T_H1/T_H17 differentiation under pathological conditions. STK40 in T cells is dispensable for immune homeostasis in resting mice. However, mice with T cell–specific deletion of STK40 exhibit attenuated symptoms of experimental autoimmune encephalomyelitis and colitis, accompanied by diminished T_H1 and T_H17 cell differentiation. Mechanistically, STK40 facilitates K48-linked polyubiquitination and proteasomal degradation of FOXO1/4 through promoting their interaction with E3 ligase COP1. Inhibition of FOXO4 or FOXO1, respectively, restores differentiation potential of STK40-deficient T_H1/T_H17 cells. Together, our data suggest a crucial role of STK40 in T_H1 and T_H17 cell differentiation, thereby enabling better understanding of the molecular regulatory network of $CD4^+$ T cell differentiation and providing effective targets for the treatment of autoimmune diseases.

INTRODUCTION

Upon recognition of a specific antigen presented by antigen-presenting cells (APCs) and receipt of the secondary signal, naïve conventional $CD4^+$ T cells enter an activation program and differentiate into functionally distinct subpopulations of effector cells based on the third signal received from various cytokines, including at least T helper 1 (T_H1), T_H2, and T_H17 cells, follicular helper T cells, and regulatory T (T_{reg}) cells, which participate in and coordinate different types of immune responses (*1*). In particular, interferon-γ (IFN-γ)–producing T_H1 cells and interleukin-17A (IL-17A)–producing T_H17 cells are required for restricting pathogen infections and mediating inflammatory and autoimmune diseases (*2*).

T_H1 and T_H17 cell differentiation is precisely modulated by multiple regulatory factors. Typically, in response to T cell receptor stimulation and IFN-γ/signal transducer and activator of transcription 1 (STAT1) signaling, naïve $CD4^+$ T cells up-regulate the expression of T-bet, the key regulator of T_H1 cell differentiation, which promotes IL-12 receptor β2 (IL-12Rβ2) expression (*3*, *4*). IL-12 binds to the IL-12R heterodimer and enhances the secretion of IFN-γ through the activation of STAT4 signaling pathway, resulting in the complete establishment of the T_H1 phenotype (*5*). Although T_H1 cells are crucial in the immune response against pathogenic infections, inappropriate T_H1 cell differentiation promotes the development of specific inflammatory diseases such as multiple sclerosis (MS) or inflammatory bowel disease (IBD) (*6*, *7*).

The pro-inflammatory cytokine IL-6, together with transforming growth factor–β (TGF-β), induces the expression of the T_H17-specific transcription factor retinoic acid–related orphan receptor γt (RORγt), which initiates the differentiation of "nonpathogenic" T_H17 that maintains homeostasis in the intestine (*8*–*10*). When further stimulated by cytokines such as IL-23 or IL-1β secreted by APCs, these cells differentiate into "pathogenic" T_H17 (pT_H17) cells (*11*), with up-regulating IL-23R and IL-1R, which promotes granulocyte-macrophage colony-stimulating factor (GM-CSF) production, induces inflammation, and promotes autoimmune diseases. Therefore, dissecting the regulatory network of T_H1 and T_H17 cell differentiation is necessary for an appropriate immune response. In addition, a critical role of the transcription factor family forkhead box O (FOXO) in the regulation of T_H cell differentiation has recently been identified. FOXO1 represses the expression of *Il17a* and *Il23r* in T_H17 cells (*12*), FOXO3a promotes T_H1 differentiation by promoting the expression of *Eomes* (*13*), whereas FOXO4 inhibits the production of IFN-γ in T_H1 cells (*14*). As an important protein posttranslational modification, ubiquitination regulates the stability and activity of FOXO proteins (*15*). Although FOXO is thought to be important in regulating T_H1 and T_H17 cells, how $CD4^+$ T cells integrate signals to regulate the activity of FOXO proteins and modulate the differentiation of T_H1 and T_H17 cells in complex immune microenvironments needs to be further investigated.

STK40, also known as Sugen kinase 495 or p65-interacting inhibitor of NF-κB (SINK)-homologous inhibitory kinase, was originally identified as a negative regulator of nuclear factor κB and p53-mediated gene transcription (*16*). The STK40 protein contains a conserved serine/threonine kinase homologous structural domain but lacks adenosine 5′-triphosphate (ATP)–binding properties and was defined as a pseudokinase (*17*). Although less well-defined, pseudokinases are found to be associated with key biological pathways that are frequently dysregulated in many diseases (*18*). The primary role of protein kinases is to catalyze the transfer of phosphoryl groups from ATP to their substrates, a process mediated by

[1]Center for Immune-Related Diseases at Shanghai Institute of Immunology, Ruijin Hospital, Shanghai Jiao Tong University School of Medicine; Hongqiao International Institute of Medicine, Shanghai Tongren Hospital, Shanghai Jiao Tong University School of Medicine; Key Laboratory of Cell Differentiation and Apoptosis of the Chinese Ministry of Education, Shanghai Jiao Tong University School of Medicine; and Shanghai Institute of Immunology, Department of Immunology and Microbiology, Shanghai Jiao Tong University School of Medicine, Shanghai, China. [2]Department of Histoembryology, Genetics and Developmental Biology, Shanghai Key Laboratory of Reproductive Medicine, Shanghai Jiao Tong University School of Medicine, Shanghai 200025, China. [3]CAS Key Laboratory of Tissue Microenvironment and Tumor, Shanghai Institute of Nutrition and Health, Chinese Academy of Sciences, Shanghai 200031, China. [4]Department of Gastroenterology, Hepatology, and Nutrition, Shanghai Children's Hospital, Shanghai Jiao Tong University, Shanghai, China.
*Corresponding author. Email: liaobing@shsmu.edu.cn (B.L.); zhangt@shchildren.com.cn (T.Z.); xuefengwu@shsmu.edu.cn (X.W.)

the folding of highly conserved kinase structural domains, but pseudokinases lack the typical phosphotransferase activity, and, thus, these enzymes retain a secondary role as effective protein scaffolds (*19*). One study showed that STK40 promotes differentiation of mouse embryonic stem cells toward the extraembryonic endoderm through activation of the extracellular signal–regulated kinase/mitogen-activated protein kinase (MAPK) pathway (*20*). Knockdown (KD) of STK40 in cultured mouse embryonic fibroblasts promotes differentiation toward adipocytes through translational control of CCAAT/enhancer binding protein β (C/EBPβ) and C/EBPδ levels (*21*). Deficiency of STK40 in mice leads to immature lung epithelial cell development, resulting in respiratory depression and perinatal death (*22*). Mechanistically, STK40 is thought to be a scaffolding protein that binds to the E3 ligase constitutively Photomorphogenic 1 (COP1), promoting substrate ubiquitination and proteasomal degradation by facilitating COP1 access to substrate proteins like c-Jun (*17*, *23*). The role of SKT40 in immune cells has been poorly investigated. Ndoja *et al.* (*24*) found that, in microglia, STK40 inhibited neuroinflammation by promoting COP1-mediated degradation of C/EBPβ. As STK40 homologous proteins, tribbles (Trib) family of pseudokinases engages in different cellular processes, including proliferation, differentiation, and metabolism (*25*). Trib proteins can also function as scaffolding molecules in a COP1-dependent manner (*26*). In addition, Trib can modulate Akt and MAPK signaling in a COP1-independent manner (*27*–*29*), yet the molecular details remain poorly understood. Several studies have elucidated the role of Trib in the immune system. *Trib1* expression is up-regulated in activated T cells, which inhibits $CD4^+$ T cell proliferation and regulates $CD8^+$ T cell differentiation during chronic infection (*30*–*32*). *Trib2*-deficient mice have subtle defects in thymic T cell development (*33*). However, the role and molecular mechanism of the pseudokinase STK40 in T cells remain to be clarified.

In this study, we reveal the critical role of STK40 in regulating T_H cell differentiation. STK40 in $CD4^+$ T cells diminishes the differentiation of T_H1 and T_H17 cells. In mouse models of acute intestinal inflammation and experimental autoimmune encephalomyelitis (EAE), STK40 deficiency attenuates T_H1- and T_H17-mediated responses, thereby delaying the disease progression. Mechanistically, we identified FOXOs as targets of STK40 to regulate T_H cell differentiation. STK40 regulates T_H1 and T_H17 cell differentiation by functioning as an adaptor protein, promoting the association between the E3 ligase COP1 and FOXO1/FOXO4, which mediates K48-linked ubiquitination and degradation of FOXO1/FOXO4 proteins via the proteasome pathway, respectively. These data suggest that ubiquitination modification of FOXO1/FOXO4 mediated by STK40 together with COP1 is essential for T_H cell differentiation.

RESULTS

STK40 expression was elevated in T cell after activation

Because *Trib1* is induced after T cell stimulation with anti-CD3/CD28 (*30*, *31*), we wondered whether STK40 is also up-regulated after T cell activation. We sorted $CD4^+$ or $CD8^+$ T cells from mouse spleen, stimulated with anti-CD3/CD28, and examined *Stk40* expression. The *Stk40* mRNA expression was up-regulated in $CD4^+$ and $CD8^+$ T cells after 4 to 6 hours of stimulation (Fig. 1, A and B), and the expression of *Stk40* was higher in $CD4^+$ T cells than that in $CD8^+$ T cells (Fig. 1C). This result implicates a role for STK40 in activated T cells. Next, we investigated the expression profile of STK40 in the $CD4^+$ T cell subsets. We sorted naïve $CD4^+$ T cells ($CD4^+CD44^{lo}CD62L^{hi}CD25^-$) from mouse spleens and induced them to differentiate into T_H1, T_H2, and T_H17 subsets under indicated conditions. The expression of *Stk40* was up-regulated in T_H1, T_H2, and T_H17 cells compared to that in naïve cells, especially in T_H1 and T_H17 cells (Fig. 1D), yet its level in T_{reg} cells was comparable to that in naïve cells (Fig. 1E). It suggests that STK40 is involved in regulating the differentiation process of T_H cells.

To investigate the role of STK40 in $CD4^+$ T cell–mediated immune response and the underlying mechanisms, we crossed $Stk40^{f/f}$ mice with *Cd4-cre* mice to generate $Stk40^{f/f}$ *Cd4-cre* ($Stk40^{\Delta T}$) mice, whose T cells were conditionally depleted of STK40 (fig. S1A). At the protein level, STK40 expression was induced in $CD4^+$ T cells upon anti-CD3/CD28, while STK40 was undetectable in $Stk40^{\Delta T}$ $CD4^+$ T cells (fig. S1B). We next analyzed the development of T cells under steady state in $Stk40^{f/f}$ and $Stk40^{\Delta T}$ mice. Eight-week-old $Stk40^{\Delta T}$ mice showed normal proportions and numbers of specific thymocyte subsets (fig. S1, C to F). In addition, percentages and numbers of $CD4^+$ and $CD8^+$ T cells in the spleen and mesenteric lymph nodes (mLNs) of $Stk40^{\Delta T}$ mice were similar to those of $Stk40^{f/f}$ mice (fig. S1, G and H). We then examined T cell homeostasis in the spleen and mLNs (Fig. 1F and fig. S1I). In the spleen, we observed that STK40 deficiency did not affect the number of effector ($CD44^{hi}CD62L^{lo}$), memory ($CD44^{hi}CD62L^{hi}$), and naïve ($CD44^{lo}CD62L^{hi}$) cells of $CD4^+$ and $CD8^+$ T cells, although there was a slight change in the proportion of memory cells in $CD4^+$ and $CD8^+$ cells of $Stk40^{\Delta T}$ mice compared to that of $Stk40^{f/f}$ mice (Fig. 1, G and H). In mLNs, loss of STK40 slightly altered percentages and numbers of memory populations in $CD4^+$ cells and $CD8^+$ cells, which had no effect on effector and naïve subsets (Fig. 1, I and J). In addition, the percentage and number of $CD4^+Foxp3^+$ T_{reg} cells in the spleen and mLNs of $Stk40^{\Delta T}$ mice were comparable to those of $Stk40^{f/f}$ mice (Fig. 1, K and L). Together, these data indicate that STK40 in T cells is dispensable for peripheral T cell homeostasis in mice under steady conditions.

STK40 promotes T_H1 and T_H17 cell differentiation

We next examined whether STK40 could regulate $CD4^+$ T cell differentiation. We purified $Stk40^{f/f}$ and $Stk40^{\Delta T}$ naïve $CD4^+$ T cells and differentiated them into T_H0, T_H1, T_H2, T_H17, pathogenic T_H17 (pT_H17), and induced T_{reg} (iT_{reg}) cells in vitro under the indicated conditions, and the lineage-specific markers were then analyzed by intracellular staining. Deletion of STK40 slightly down-regulated IFN-γ expression in T_H0 cells and significantly decreased IFN-γ expression in T_H1 cells (Fig. 2, A and B). In addition, STK40 deficiency impaired IL-17A expression in T_H17 and pT_H17 cells (Fig. 2, C and D). Because pathogenic T_H17 cells can produce IFN-γ, which demonstrates enhanced pathogenicity, we examined the expression of IFN-γ in T_H17 and pT_H17 cells, and the results showed that deletion of STK40 lowered percentages of IFN-γ–producing cells among pT_H17 cells (fig. S2, A and B), implying attenuation of the pathogenicity of STK40-deficient pT_H17 cells. In addition, STK40 depletion had no effect on IL-4 and Foxp3 expression in T_H2 and iT_{reg} cells, respectively (fig. S2, C and D). Furthermore, consistent with the above results, enzyme-linked immunosorbent assay (ELISA) results showed that STK40-deficient T_H0 cells produced less IFN-γ and IL-17A (Fig. 2, E and F), and STK40-deficient T_H1 and pT_H17 cells down-regulated the production of IFN-γ and IL-17A, respectively (Fig. 2, G and H). Although numbers of lamina propria lymphocytes from the colon and small intestine of $Stk40^{f/f}$ and $Stk40^{\Delta T}$

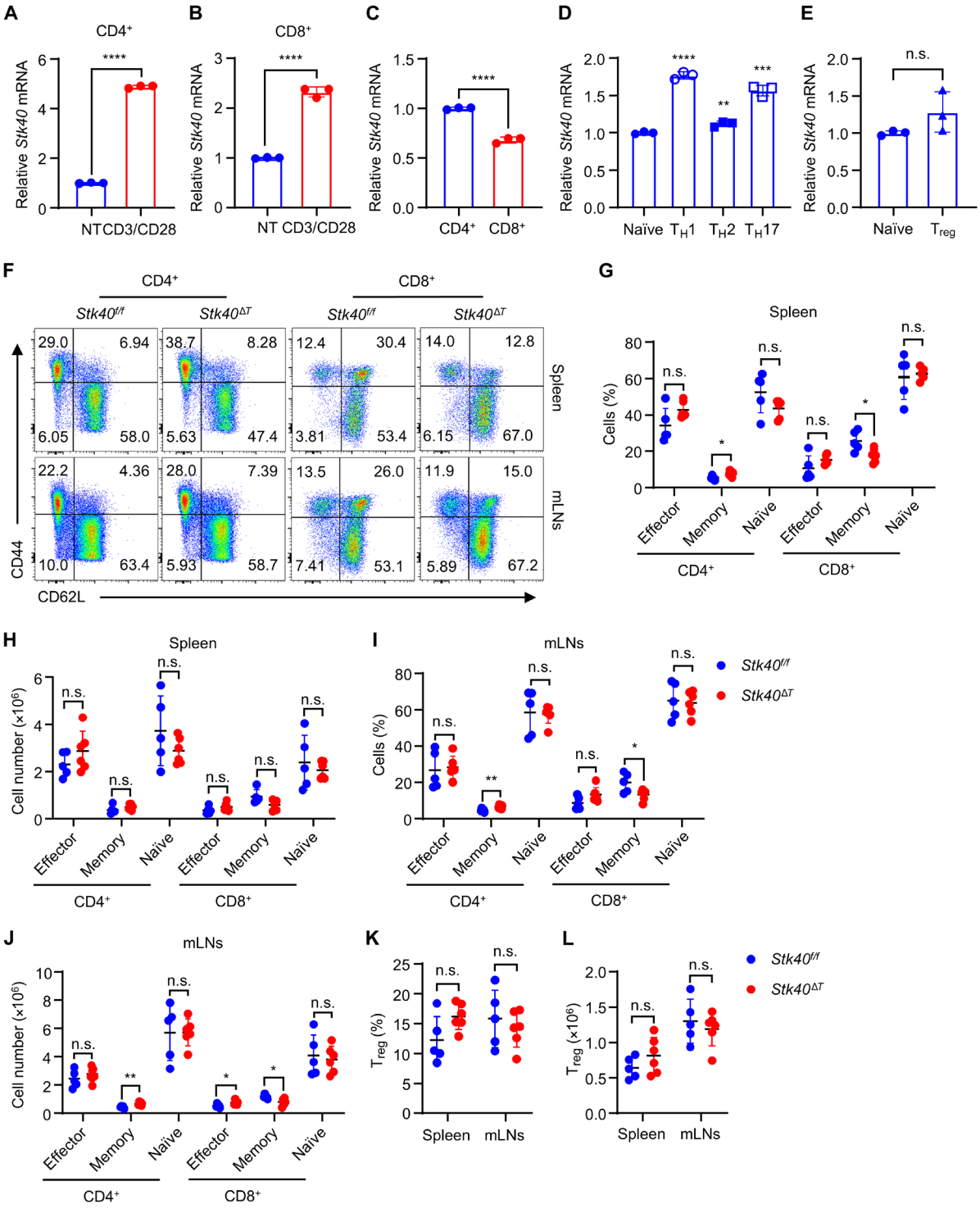

Fig. 1. STK40 expression is elevated in activated T cells. (**A** to **C**) Reverse transcription quantitative polymerase chain reaction (qPCR) analysis of relative *Stk40* mRNA expression in [(A) and (C)] $CD4^+$ T cells and [(B) and (C)] $CD8^+$ T cells sorted from spleens and lymph nodes of mice following 4 hours ± anti-CD3/CD28 stimulation ($n = 3$). (**D**) qPCR analysis of Stk40 mRNA expression in naïve, T_H1, T_H2, and T_H17 cells ($n = 3$). (**E**) qPCR analysis of relative *Stk40* mRNA expression in naïve $CD4^+$ T cells and T_{reg} cells sorted from spleens and lymph nodes of mice ($n = 3$). (**F**) Flow cytometry plot for $CD62L^{lo}CD44^{hi}$ (effector), $CD62L^{hi}CD44^{hi}$ (memory), and $CD62L^{hi}CD44^{lo}$ (naïve) cells of $CD4^+$ or $CD8^+$ T cells in spleens and mesenteric lymph nodes (mLNs) of $Stk40^{f/f}$ and $Stk40^{\Delta T}$ mice ($n = 5$ to 6). (**G** to **J**) Statistics of percentages [(G) and (I)] and numbers [(H) and (J)] of $CD62L^{lo}CD44^{hi}$ (effector), $CD62L^{hi}CD44^{hi}$ (memory), and $CD62L^{hi}CD44^{lo}$ (naïve) cells among $CD4^+$ or $CD8^+$ T cells in spleens and mLNs of $Stk40^{f/f}$ and $Stk40^{\Delta T}$ mice ($n = 5$ to 6). (**K** and **L**) Statistics of percentages (K) and numbers (L) of $Foxp3^+$ (T_{reg}) among $CD4^+$ T cells in spleens and mLNs of $Stk40^{f/f}$ and $Stk40^{\Delta T}$ mice ($n = 5$ to 6). Data are presented as means ± SD. $^*P < 0.05$; $^{**}P < 0.01$; $^{***}P < 0.001$; $^{****}P < 0.0001$; n.s., not significant (Student's *t* test). All data presented in this panel are the result of at least three independent experiments.

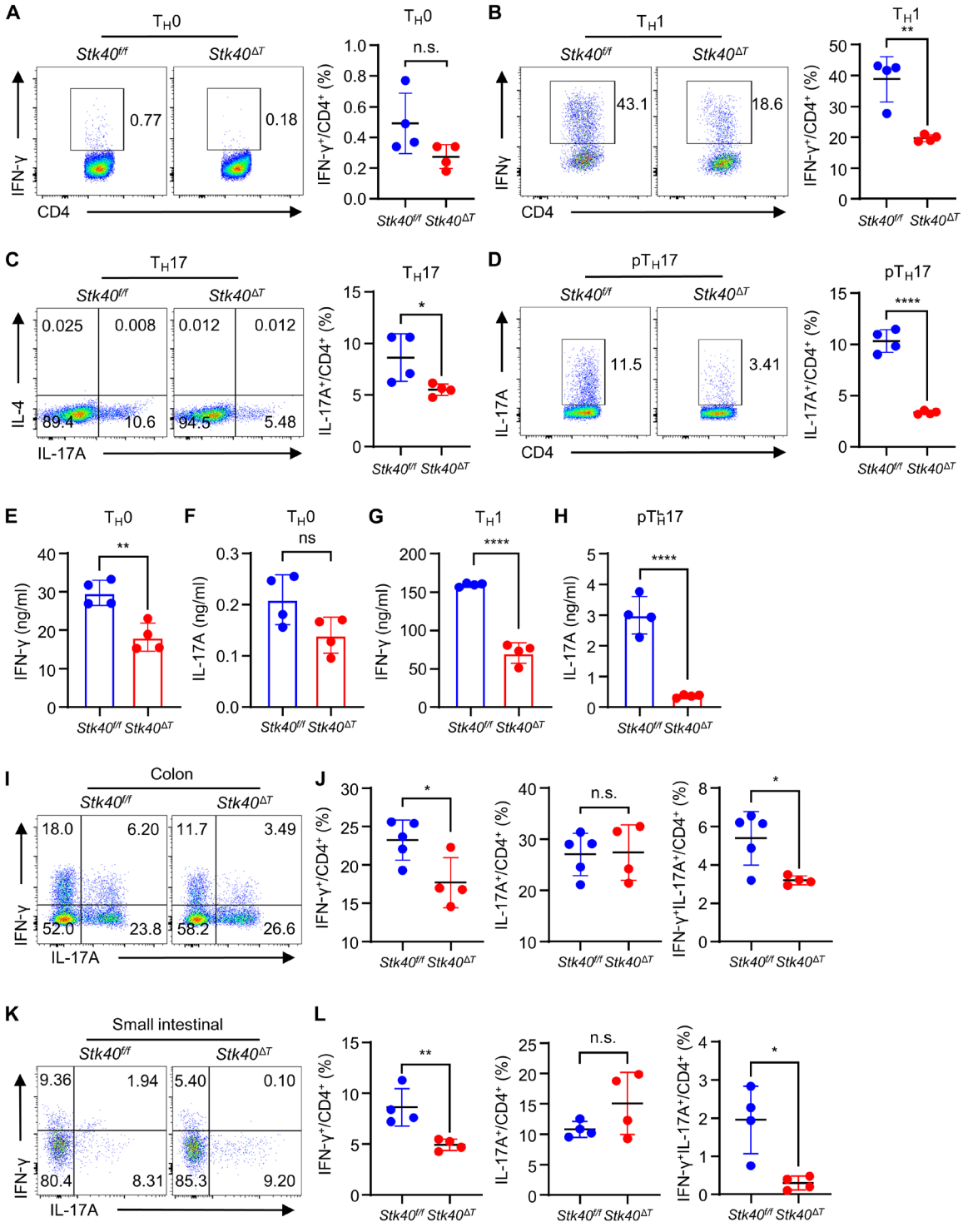

Fig. 2. STK40 promotes T_H1 and T_H17 cell differentiation. (**A** to **D**) Flow cytometry plot (left) and analysis (right) of the frequency of IFN-γ$^+$ or IL-17A$^+$ cells in differentiated T_H0 (A), T_H1 (B), T_H17 (C), and pT_H17 (D) for 3 days of *Stk40*$^{f/f}$ and *Stk40*$^{\Delta T}$ mice ($n = 4$). (**E** and **F**) Supernatants of differentiated *Stk40*$^{f/f}$ and *Stk40*$^{\Delta T}$ T_H0 cells for 3 days were collected and the levels of IFN-γ and IL-17A were measured by enzyme-linked immunosorbent assay (ELISA; $n = 4$). (**G** and **H**) Supernatants of differentiated *Stk40*$^{f/f}$ and *Stk40*$^{\Delta T}$ T_H1 and pT_H17 cells for 3 days were collected, and the levels of IFN-γ or IL-17A were measured by ELISA ($n = 4$). (**I** and **J**) Flow cytometry plot (I) and analysis (J) for the frequency of IFN-γ$^+$ and IL-17A$^+$CD4$^+$ T cells in colonic lamina propria separated from *Stk40*$^{f/f}$ and *Stk40*$^{\Delta T}$ mice ($n = 4$ to 5). (**K** and **L**) Flow cytometry plot (K) and analysis (L) for the frequency of IFN-γ$^+$ and IL-17A$^+$CD4$^+$ T cells in the lamina propria of small intestine separated from *Stk40*$^{f/f}$ and *Stk40*$^{\Delta T}$ mice ($n = 4$). Data are presented as means ± SD. *$P < 0.05$; **$P < 0.001$; ****$P < 0.0001$ (Student's *t* test). All data presented in this panel are the result of at least three independent experiments.

mice at steady state were similar, STK40 deletion resulted in a down-regulation of the proportion of IFN-γ^+ and IFN-γ^+IL-17A$^+$ cells of CD4$^+$ T cells in the lamina propria (Fig. 2, I to L, and fig. S2, E to G). In CD8$^+$ T cells from the lamina propria, loss of STK40 did not affect the proportions of IFN-γ^+ and IL-17A$^+$ cells; however, STK40 deficiency led to an up-regulation of the number of IFN-γ^+ expressing CD8$^+$ T cells in the lamina propria of the small intestine (fig. S2, H and I), which may be due to a compensatory mechanism for maintaining homeostasis. Because the presence of gut microbes in colon can induce differentiation of T_H1 (*34*), these findings suggest that absence of STK40 impaired T_H1 differentiation in vivo. Besides, we detected that STK40 did not affect the proliferative capacity of T_H1 and T_H17 cells (fig. S2J). Together, these results reveal that STK40 is essential for T_H1 and T_H17 cell differentiation.

Deletion of STK40 in T cells alleviated DSS-induced colitis in mice

Up-regulation of IL-12 cytokine family such as IL-12 and IL-23 in IBD controls the infiltration of T_H1 and T_H17 cells in the inflamed gut, which is a sign of the IBD (*35*). Although T_H17 cells in the gut can play a protective and homeostatic role, they can also mediate intestinal pathology (*36*). Increasing evidence suggests that CD4$^+$ T cells are involved in the pathogenesis of IBD by up-regulating the expression of pro-inflammatory cytokines such as IFN-γ, tumor necrosis factor (TNF), and IL-17A (*37*). The above results showed that STK40 deletion in T cells resulted in altered stability of homeostatic T_H1 cells in the mice intestine, but we did not observe any change in the proportion of IL-17A$^+$ cells (Fig. 2, I to L). We used an acute colitis mouse model to investigate the effects of STK40 on inflammatory T_H1 and T_H17 cells under pathologic conditions. Compared with *Stk40*$^{f/f}$ mice, *Stk40*$^{\Delta T}$ mice showed less weight loss and longer colon length after dextran sulfate sodium (DSS)–containing water feeding (Fig. 3, A to C). Histopathologic hematoxylin and eosin (H&E) staining demonstrated that STK40 deficiency in T cells reduced inflammatory cell infiltration and caused less mucosal epithelial destruction after DSS treatment (Fig. 3D). Flow cytometric analysis identified reduction of IFN-γ^+, IL-17A$^+$, and TNF$^+$CD4$^+$ T cells in the inflamed colon of *Stk40*$^{\Delta T}$ mice (Fig. 3, E and F, and fig. S3, A and B) but unchanged cytokine-production in CD8$^+$ T cells (fig. S3, C and D). Collectively, these data suggest that STK40 promotes T_H1- and T_H17-mediated intestinal immune responses in acute murine colitis.

Loss of STK40 in T cell ameliorates T cell–mediated chronic colitis in mice

To obtain better insight into the intrinsic function of STK40 in the CD4$^+$ T cell–mediated chronic inflammation and autoimmune

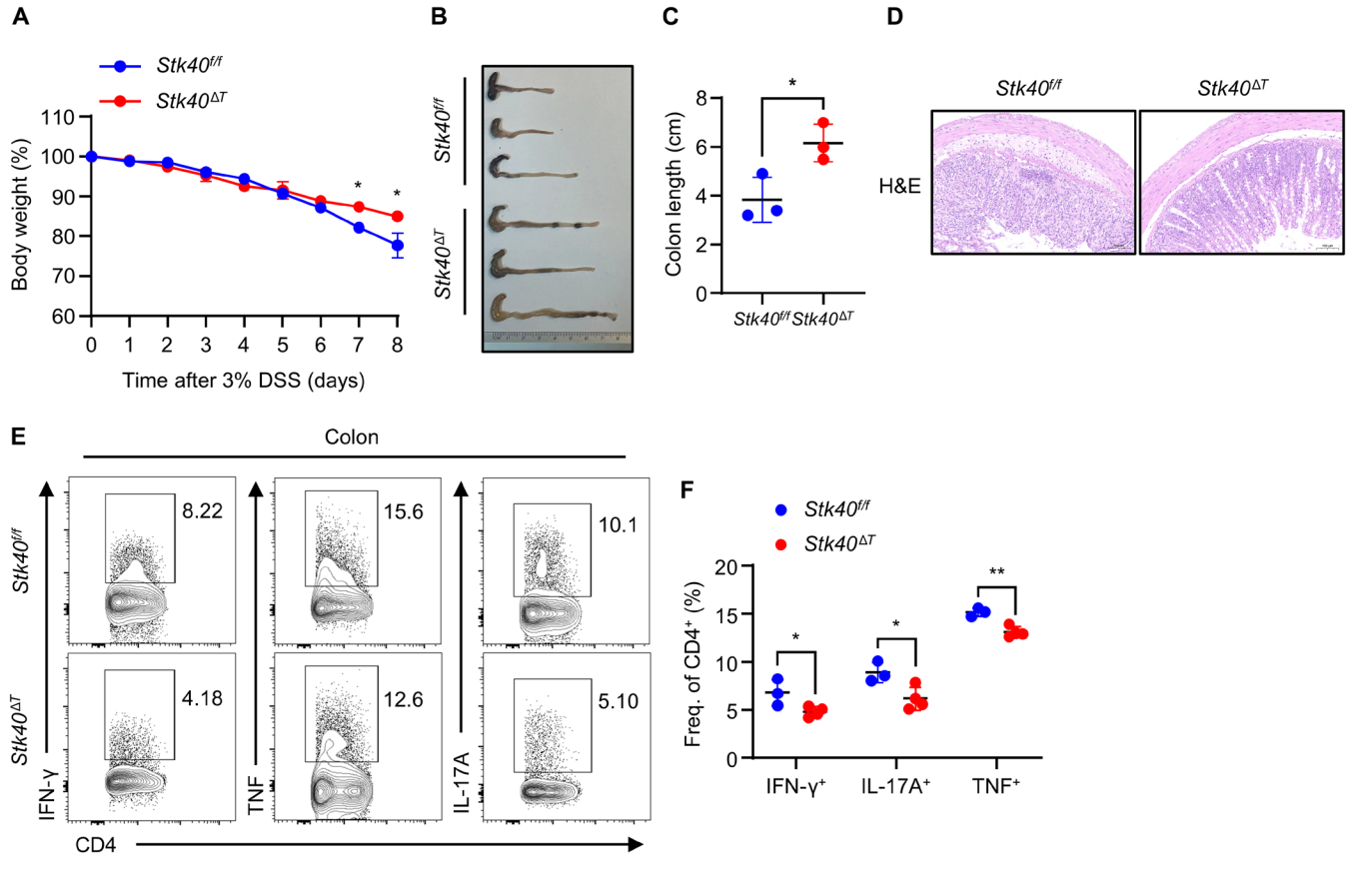

Fig. 3. Deletion of STK40 in T cells alleviates DSS-induced colitis in mice. (**A**) Weight changes of *Stk40*$^{f/f}$ and *Stk40*$^{\Delta T}$ mice challenged with 3% DSS in drinking water for 8 days ($n = 5$). (**B**) Gross morphology of the large bowels on the eighth day after DSS exposure in *Stk40*$^{f/f}$ and *Stk40*$^{\Delta T}$ mice ($n = 3$). (**C**) Summarized colonic lengths of DSS-treated *Stk40*$^{f/f}$ and *Stk40*$^{\Delta T}$ mice harvested on day 8 ($n = 3$). (**D**) Hematoxylin and eosin (H&E) staining for *Stk40*$^{f/f}$ and *Stk40*$^{\Delta T}$ mice colon after DSS treatment. (**E** and **F**) Flow cytometry plot (E) and analysis (F) for the frequency of IFN-γ^+, IL-17A$^+$ and TNF$^+$ CD4$^+$ T cells in colonic lamina propria separated from DSS-treated *Stk40*$^{f/f}$ and *Stk40*$^{\Delta T}$ mice ($n = 3$). Data are presented as means ± SD. *$P < 0.05$ (Student's *t* test). All data presented in this panel are the result of at least two independent experiments.

diseases, we used a T cell transfer colitis model. Naïve $CD4^+$ T cells ($CD4^+CD45RB^{hi}CD25^-$) from *Stk40*$^{f/f}$ or *Stk40*$^{\Delta T}$ mice were transferred into *Rag2*$^{-/-}$ mice to induce colitis. Mice transferred with *Stk40*$^{f/f}$ $CD4^+$ T cells lost significantly more weight and had shorter colons compared to mice transferred with STK40-deficient $CD4^+$ T cells (Fig. 4, A to C). Compared with *Rag2*$^{-/-}$ mice transferred with wild-type (WT) $CD4^+$ T cells, *Rag2*$^{-/-}$ mice transferred with STK40-deficient $CD4^+$ T cells displayed much milder colitis symptoms, as shown by histologic examination of colon sections (Fig. 4D), fewer $CD4^+$ T cell infiltration, as shown by flow cytometry and immunofluorescence staining (Fig. 4, E and F), and decreased percentage and number of IFN-γ^+CD4^+ T cells (Fig 4G). To summarize, these results suggest that T cell–intrinsic STK40 is important for T cell–mediated chronic colitis in mice.

STK40 deficiency in T cells ameliorates EAE

MS is a central nervous system (CNS) autoimmune disease mediated primarily by autoreactive T_H1 and T_H17 cells (*38*). Given that STK40

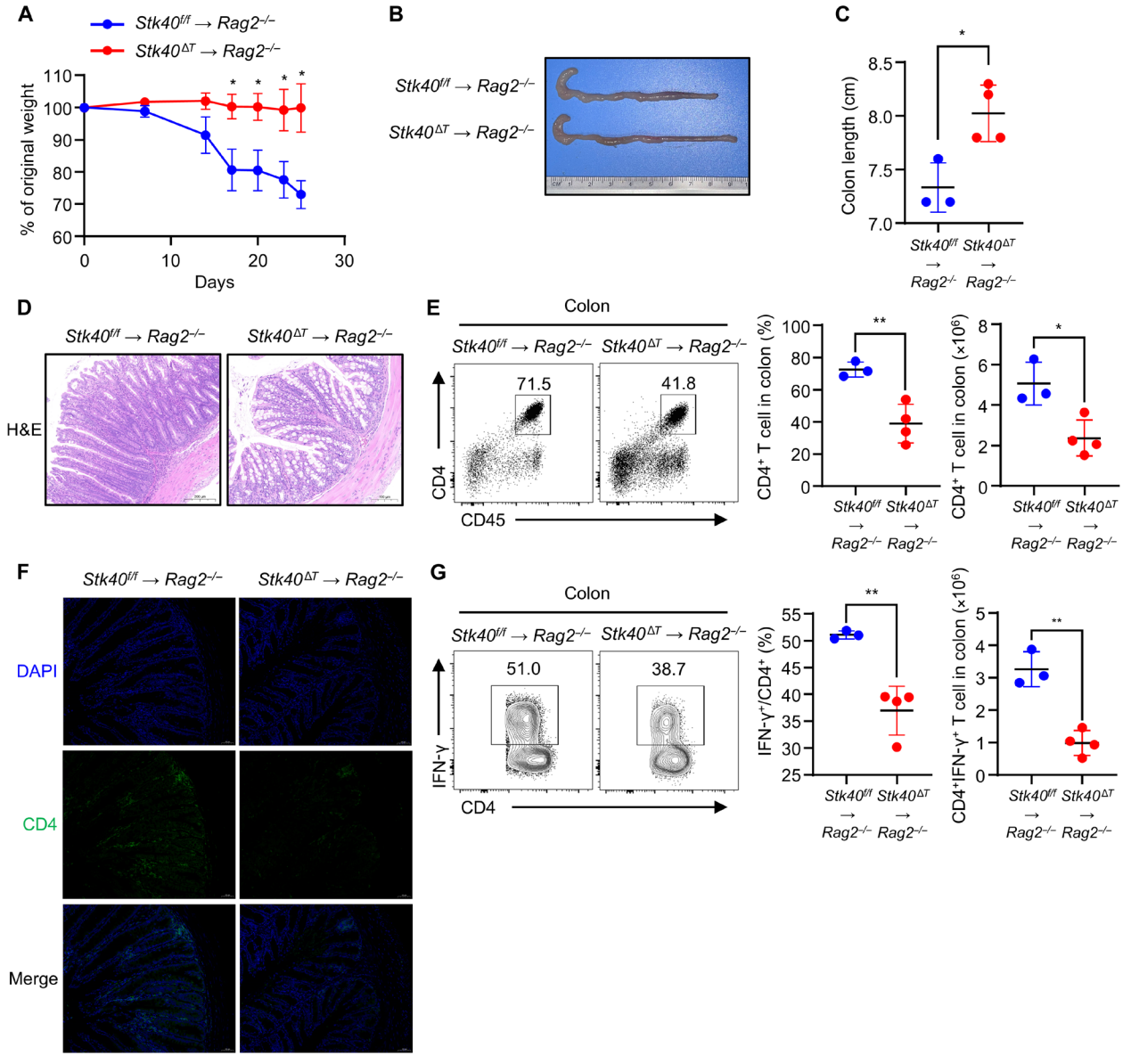

Fig. 4. Loss of STK40 in T cell ameliorates T cell–mediated chronic colitis in mice. (**A**) Naïve $CD4^+$ T cells (5×10^5) from *Stk40*$^{f/f}$ or *Stk40*$^{\Delta T}$ mice were isolated and transferred into *Rag2*$^{-/-}$ mice. The body weights of recipient mice were measured weekly ($n = 4$ to 5). (**B**) Representative photograph of the colons of mice from (A) obtained at 4 weeks after the adoptive transfer colitis model. (**C**) Summarized colonic lengths of mice from (A) obtained at 4 weeks after the adoptive transfer colitis model ($n = 3$ to 4). (**D**) H&E staining for the colon sections of *Rag2*$^{-/-}$ mice transferred with *Stk40*$^{f/f}$ or *Stk40*$^{\Delta T}$ naïve $CD4^+$ T cells. (**E**) Flow cytometry plot (left) and analysis (right) for the percentage and number of $CD4^+$ T cells in the colon of *Rag2*$^{-/-}$ recipient mice at 4 weeks after T cell transfer ($n = 3$ to 4). (**F**) Representative CD4 (green) immunofluorescence analysis of colon sections. DAPI, 4′,6-diamidino-2-phenylindole. (**G**) Flow cytometry plot (left) and analysis (right) for the percentage and number of IFN-γ^+CD4^+ T cells in the colon of *Rag2*$^{-/-}$ recipient mice at 4 weeks after T cell transfer ($n = 3$ to 4). Data are presented as means ± SD. *$P < 0.05$; **$P < 0.01$ (Student's *t* test).

promotes T_H1 and T_H17 cell differentiation, we investigated the in vivo role of STK40 in regulating EAE, an established mouse model of human MS (*39*). We immunized *Stk40*$^{f/f}$ and *Stk40*$^{\Delta T}$ mice with myelin oligodendrocyte glycoprotein (MOG_{35-55}) peptide to trigger EAE, STK40 deficiency in T cells delayed the onset of disease and reduced the severity at the peak of the disease (Fig. 5, A and B), and *Stk40*$^{\Delta T}$ mice lost less weight during EAE (Fig. 5C). Histopathological analysis revealed less inflammation and less destruction of myelin in the spinal cord of *Stk40*$^{\Delta T}$ mice compared to that of *Stk40*$^{f/f}$ mice at the peak of EAE (Fig. 5D). Moreover, the number of CNS-infiltrated mononuclear cells and the proportion and number of CD45$^+$ cells were significantly reduced in *Stk40*$^{\Delta T}$ EAE mice (Fig. 5, E and F,

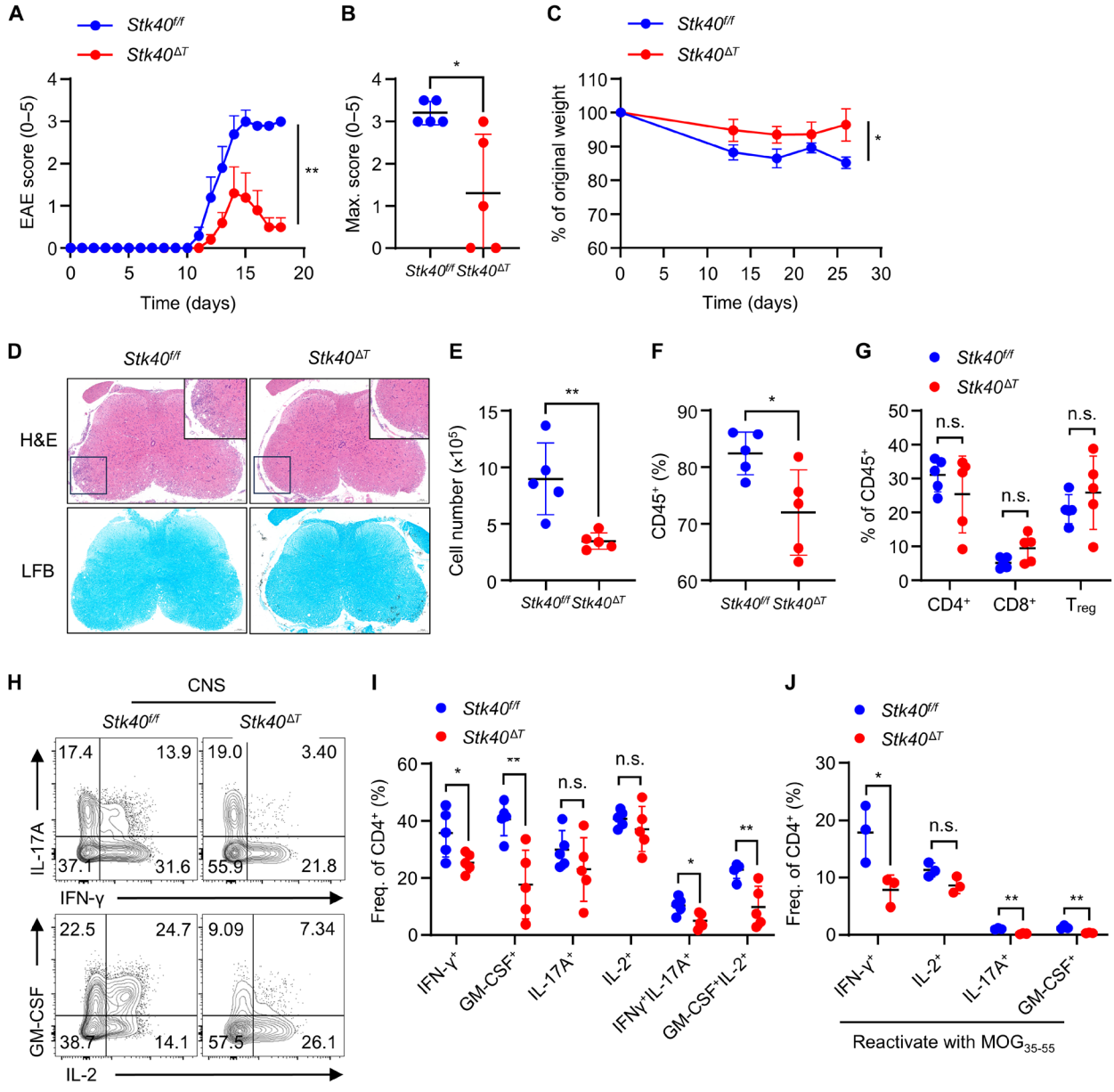

Fig. 5. STK40 deficiency in T cells ameliorates EAE. (**A**) *Stk40*$^{f/f}$ and *Stk40*$^{\Delta T}$ mice were immunized with MOG_{35-55} and monitored daily for clinical signs ($n = 5$). (**B**) Maximum (Max.) EAE clinical scores reached for each individual mouse during the observation period from (A). (**C**) Body weight loss of *Stk40*$^{f/f}$ and *Stk40*$^{\Delta T}$ mice after immunized with MOG_{35-55} ($n = 5$). (**D**) Representative histopathological sections of spinal cords from mice at the peak EAE, showing immune cell infiltration via H&E staining and demyelination via Luxol fast blue (LFB) staining. (**E**) Total number of infiltrating mononuclear cells in the CNS from mice at the peak of EAE ($n = 5$). (**F**) Statistics of the proportion of infiltrating CD45$^+$ cells in the CNS from mice at the peak of EAE ($n = 5$). (**G**) Statistics of the proportion of infiltrating CD4$^+$ and CD8$^+$ T cells and T_{reg} cells among CD45$^+$ cells in the CNS from mice at the peak of EAE ($n = 5$). (**H** and **I**) Flow cytometry plot (H) and analysis (I) of frequencies of IFN-γ$^+$, GM-CSF$^+$, IL-17A$^+$, IL-2$^+$, IFN-γ$^+$IL-17A$^+$, and GM-CSF$^+$IL-2$^+$ cells of CD4$^+$ T cells in the CNS from mice at the peak of EAE ($n = 5$). (**J**) Statistics of the proportion of IFN-γ$^+$, IL-2$^+$, IL-17A$^+$, and GM-CSF$^+$ of CD4$^+$ cells in reactivated splenocytes from mice at the onset of EAE ($n = 3$). The data in (A) are presented as the means ± SEM, and statistical differences in (A) and (B) were tested by nonparametric Mann-Whitney test. The data in (C), (E) to (G), and (I) and (J) are presented as the means ± SD, and statistical differences were tested using unpaired Student's *t* test (two-tailed). *$P < 0.05$; **$P < 0.01$. All data presented in this panel are the result of at least three independent experiments.

and fig. S4, A and B). In CNS-infiltrated immune cells, T cell–specific STK40 ablation did not alter percentages of $CD4^+$, $CD8^+$, and T_{reg} cells, whereas the numbers of $CD4^+$ cells and T_{reg} cells were down-regulated (Fig. 5G and fig. S4C). We next analyzed the response of T cells infiltrated in the CNS at the peak of EAE, and the results showed that $CD4^+$ T cells expressing T_H1- and T_H17-related cytokines (IFN-γ, GM-CSF, IL-17A, and IL-2) and transcription factors (T-bet, RORγt, and Eomes) were reduced in *Stk40*$^{\Delta T}$ mice compared with those in *Stk40*$^{f/f}$ mice (Fig. 5, H and I, and fig. S4, D to F). In addition, in draining lymph nodes of *Stk40*$^{\Delta T}$ mice, the proportion of $CD4^+$ T cells expressing T-bet and RORγt was down-regulated (fig. S4G), whereas the percentage and number of cytokine-producing $CD8^+$ T cells were not altered (fig. S4, H and I). In addition, we harvested splenocytes from immunized mice on day 10 and restimulated them in vitro with MOG_{35-55} peptide and found that $CD4^+$ T cells from splenocytes of *Stk40*$^{\Delta T}$ mice contained fewer pro-inflammatory cytokines such as IFN-γ–, IL-17A–, and GM-CSF–producing cells compared to those of *Stk40*$^{f/f}$ mice (Fig. 5J). Furthermore, at the peak of EAE, *Stk40*$^{\Delta T}$ mice had a lower proportion and number of innate immune cells, such as macrophages ($CD11b^+F4/80^+$) and dendritic cells ($CD11c^+$), that infiltrated the CNS in response to cytokine production by T_H1 and T_H17 cells (*40*), while there was no change in the proportion and number of neutrophils ($CD11b^+Ly6G^+$) (fig. S4, J to L). Together, our findings suggest that STK40 mediates autoimmune inflammation in mice by promoting polarization of T_H1 and T_H17 cells.

STK40 deficiency leads to loss of the expression of central regulatory genes in T_H1 and T_H17 cells

Considering that STK40 stably promotes T_H1 differentiation, we sorted naïve $CD4^+$ T cells from the spleens of *Stk40*$^{f/f}$ and *Stk40*$^{\Delta T}$ mice and cultured for 3 days under T_H1-polarized conditions, followed by bulk RNA sequencing (RNA-seq) analysis. Compared to WT controls, STK40-deficient T_H1 cells exhibited up-regulation of 2787 genes and down-regulation of 1932 genes (Fig. 6A). T_H1 cells with a deficit in STK40 down-regulated the expression of key transcription factors and cytokine genes such as *Tbx21*, *Eomes*, *Ifng*, and *Csf2* of T_H1 cell at the transcriptional level (Fig. 6B). Enrichment analysis of differentially expressed genes by the Gene Ontology and Kyoto Encyclopedia of Genes and Genomes pathway revealed that pathways related to cell differentiation and immune responses and pathways associated with autoimmune-related diseases such as IBD and rheumatoid arthritis were down-regulated in T_H1 cells lacking STK40 (Fig. 6C). Reverse transcription quantitative polymerase chain reaction (qPCR) analysis confirmed that STK40 deficiency markedly down-regulated *Ifng*, *Tbx21*, and *Csf2* expression in T_H1 cells (Fig. 6D). Meanwhile, we performed qPCR analysis of T_H17 cells induced in vitro, and the data showed that the expression of the signature factor *Il17a* gene and the key transcription factor *Rorc* gene was down-regulated in the absence of STK40, and the expression of genes contributing to T_H17 differentiation, such as *Il23r* and *Rora*, was also down-regulated (Fig. 6E). Collectively, these results suggest that STK40 maintains the expression of a broad range of T_H1 and T_H17 signature genes.

STK40 up-regulates T_H1 differentiation by inhibiting FOXO4

The above results prompted us to explore the underlying mechanisms by which STK40 regulates T_H1 cell differentiation. On the basis of the data from RNA-seq, we found that the FoxO signaling pathway was up-regulated in STK40-deficient T_H1 cells (Fig. 7, A and B). FOXO family of transcription factors is involved in the regulation of various intracellular activities such as cellular resistance to oxidative stress, cell proliferation, apoptosis, autophagy, and metabolism (*41*, *42*). FOXO1, together with another FOXO family member FOXO3a, regulates T_{reg} formation by binding to the promoter region of the *Foxp3* gene (*43*, *44*). FOXO1 can also inhibit the differentiation of T_H17 cells by inhibiting binding of RORγt to its target gene (*12*). FOXO3a promotes T_H1 differentiation by inducing the expression of Eomes (*13*). In contrast, FOXO4 inhibited IFN-γ production in T_H1 cells by targeting Dkk3 and down-regulating its downstream lymphoid enhancer binding factor 1 expression (*14*). Therefore, we examined the expression of FOXO1, FOXO3a, and FOXO4 mRNA and proteins in T_H1 cells; the results demonstrated that STK40 deletion did not affect their expression at the transcriptional (fig. S5A), and STK40-deficient T_H1 cells have normal protein levels of FOXO1 and FOXO3a, while the expression of FOXO4 is significantly up-regulated (Fig. 7, C to E). To further confirm the regulation of FOXO4 protein by STK40, we constructed Jurkat cell lines with KD of STK40 or STK40 overexpression (OE) using a lentiviral infection system (fig. S5, B and C). Immunoblotting showed that FOXO4 expression was up-regulated in KD Jurkat cells compared to that in Jurkat cells transfected with scramble short hairpin RNA (shRNA) (SCR), while FOXO4 expression was down-regulated in OE Jurkat cells (Fig. 7, F and G), all consistent with the observation in mouse T_H1 cells. These results indicate that STK40 inhibits the expression of FOXO4 at the protein level in T_H1 cells.

To confirm that STK40 promotes T_H1 differentiation by inhibiting FOXO4 expression, we assessed whether KD of FOXO4 eliminates the T_H1 inhibition associated with STK40 deficiency. We first treated *Stk40*$^{\Delta T}$ T_H1 cells with *Foxo4* small interfering RNA (siRNA), which resulted in effective down-regulation of FOXO4 protein (fig. S5D). Then, by flow cytometry, ELISA, and qPCR analysis, we found that silencing FOXO4 promoted IFN-γ production by *Stk40*$^{\Delta T}$ T_H1 cells to a level close to that observed in *Stk40*$^{f/f}$ cells (Fig. 7, H and I, and fig. S5, E and F). In addition, qPCR analysis and flow cytometry revealed that KD of FOXO4 up-regulated the expression of T-bet to a level close to normal in STK40-deficient T_H1 cells (fig. S5, G to I). In conclusion, these results suggest that STK40 promotes T_H1 induction by targeting FOXO4.

STK40 promotes K48-linked polyubiquitination of FOXO4 through E3 ligase COP1

Next, we wondered how exactly STK40 regulates the expression of FOXO4 protein. First, we transfected the hemagglutinin (HA)–tagged STK40 plasmid together with the Flag-tagged FOXO4 plasmid into human embryonic kidney (HEK) 293T cells and performed co-immunoprecipitation (co-IP) experiments. The results showed that STK40 interacted with FOXO4 (Fig. 8A). Previous studies have shown that FOXO4 is a substrate for the E3 ubiquitin ligase COP1 (*45*). STK40 is regarded as a scaffolding protein that facilitates the binding of COP1 to the substrate to promote its ubiquitination and degradation by the proteasome (*23*). Thus, we hypothesized that STK40 binds FOXO4 to regulates its ubiquitination and degradation by COP1. We first treated SCR and STK40-OE Jurkat cells with the proteasome inhibitor MG132 to confirm STK40 promotes the degradation of FOXO4 protein through proteasome pathway. The results showed that the MG132-treated SCR and STK40-OE Jurkat

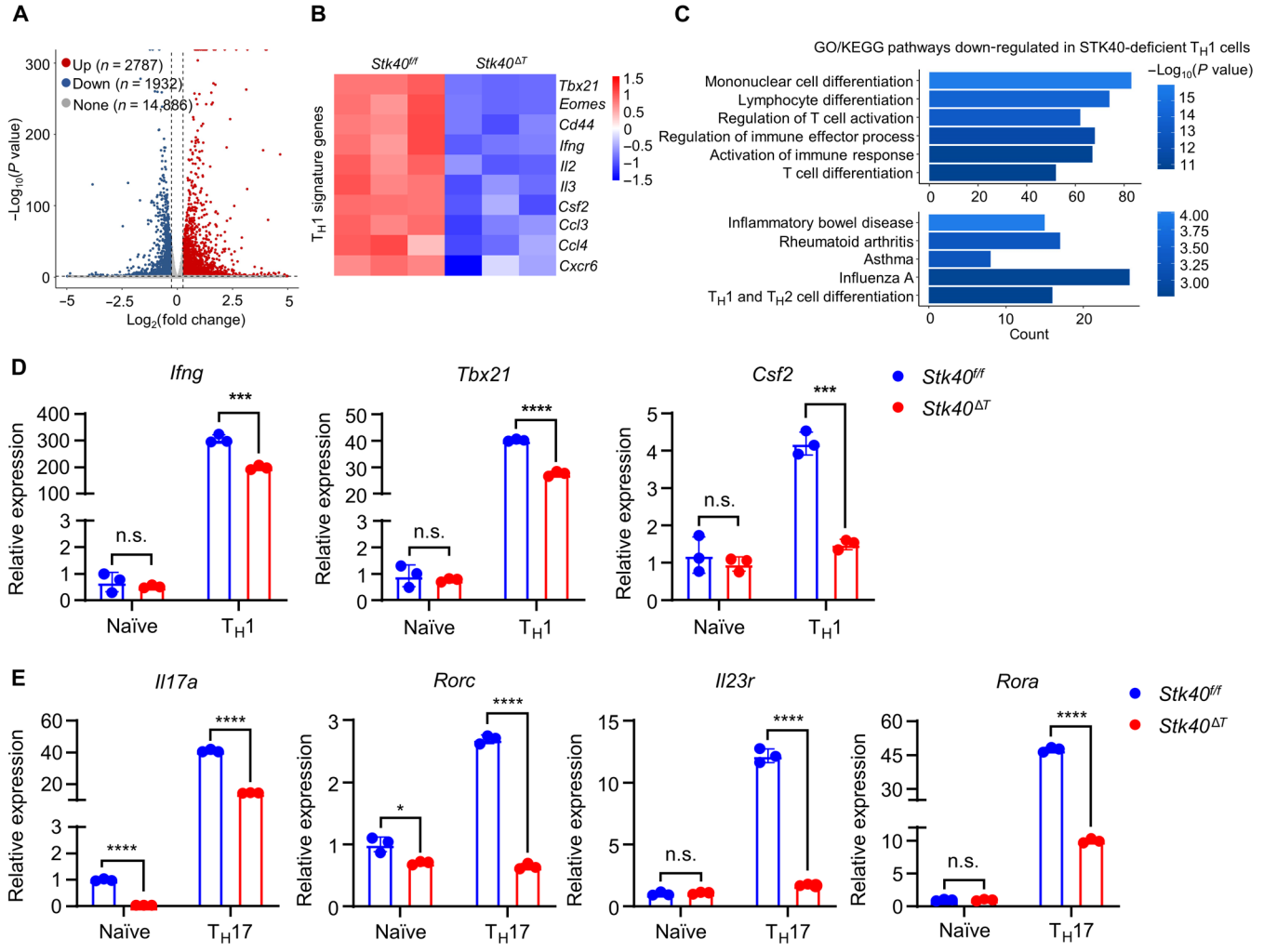

Fig. 6. STK40 deficiency leads to loss of the expression of central regulatory genes in T_H1 and T_H17 cells. (**A**) Scatterplot comparing global gene expression profiles of *Stk40*$^{f/f}$ and *Stk40*$^{\Delta T}$ naïve CD4$^+$ T cells cultured under T_H1-polarizing conditions for 3 days. Genes significantly ($P < 0.05$) up-regulated and down-regulated are depicted in red and blue, respectively. (**B**) Clustering of differentially expressed T_H1 signature genes identified in T_H1 cells from *Stk40*$^{f/f}$ and *Stk40*$^{\Delta T}$ mice. Red and blue represent high and low levels of expression of indicated genes, respectively. The colors indicate the value of $\log_2$ fold change. (**C**) Functional enrichment analysis of Kyoto Encyclopedia of Genes and Genomes (KEGG) and Gene Ontology (GO) pathways down-regulated in *Stk40*$^{\Delta T}$ T_H1 cells compared with *Stk40*$^{f/f}$ cells. (**D**) qPCR analysis of relative mRNA expression of indicated genes in *Stk40*$^{f/f}$ and *Stk40*$^{\Delta T}$ naïve CD4$^+$ T cells cultured under T_H1-polarizing conditions for 3 days ($n = 3$). (**E**) qPCR analysis of relative mRNA expression of indicated genes in *Stk40*$^{f/f}$ and *Stk40*$^{\Delta T}$ naïve CD4$^+$ T cells cultured under T_H17-polarizing conditions for 3 days ($n = 3$). Data are presented as means ± SD. *$P < 0.05$; ***$P < 0.001$; ****$P < 0.0001$ (Student's *t* test). All data presented in this panel are the result of at least three independent experiments.

cells exhibited marked accumulation of FOXO4 protein compared to the dimethyl sulfoxide–treated group (Fig. 8B). Next, using co-IP assays, we demonstrated that the interaction between FOXO4 and COP1 is enhanced in the presence of STK40 (Fig. 8C). To further determine that STK40 regulates the proteasome-mediated degradation of FOXO4 protein, we analyzed the FOXO4 K48-linked ubiquitination levels in the presence or absence of STK40. Results showed that STK40 OE significantly up-regulated the level of FOXO4 K48-linked ubiquitination in HEK293T cells (Fig. 8D). Last, consistent with our speculation, OE of COP1 promotes the ubiquitination of FOXO4, and OE of STK40 exacerbates this effect (Fig. 8E). Together, our findings suggest that STK40 down-regulates the level of FOXO4 by promoting K48-linked ubiquitination and proteasomal degradation of FOXO4 protein through COP1, thereby promoting differentiation of Th1 cells.

STK40 up-regulates T_H17 cell differentiation through facilitating COP1-mediated K48-linked polyubiquitination of FOXO1

Previous studies showed that FOXO4 only affects the differentiation of T_H1 cells but has no notable effect on T_H2, T_H17, and T_{reg} cells (*14*). Therefore, we wondered how STK40 regulates T_H17 cell differentiation. Another member of the FOXO family, FOXO1, is thought to play an essential role in the regulation of non-pathological or pathological T_H17 cells. In addition, it has been shown that FOXO1 is also a substrate for ubiquitination of COP1 (*46*). Thus, we

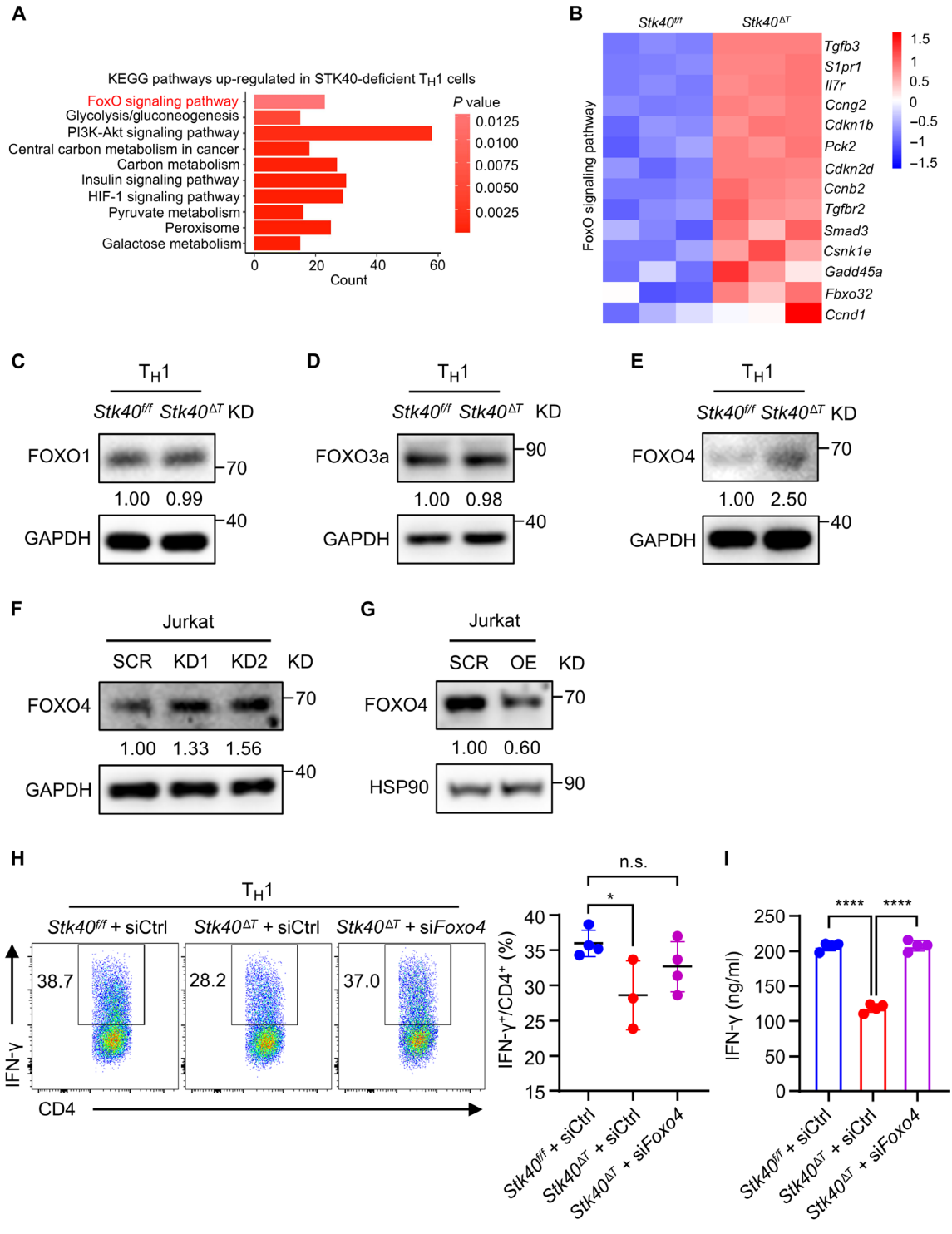

Fig. 7. STK40 up-regulates T_H1 differentiation by inhibiting FOXO4. (**A**) Functional enrichment analysis of KEGG and GO pathways up-regulated (red bars) in *Stk40*$^{\Delta T}$ T_H1 cells compared with *Stk40*$^{f/f}$ cells. HIF-1, hypoxia-inducible factor 1. (**B**) Clustering of differentially expressed FoxO signaling pathway related genes identified in T_H1 cells from *Stk40*$^{f/f}$ and *Stk40*$^{\Delta T}$ mice. Red and blue represent high and low levels of expression of indicated genes, respectively. The colors indicate the value of log2 fold change. (**C** to **E**) Immunoblot analysis of FOXO1 (C), FOXO3a (D), and FOXO4 (E) proteins in *Stk40*$^{f/f}$ and *Stk40*$^{\Delta T}$ T_H1 cells. (**F** and **G**) Immunoblot analysis of the FOXO4 in scramble (SCR) and shSTK40 (KD) (F) or in SCR and STK40-overexpression (OE) (G) Jurkat T cells. GAPDH, glyceraldehyde-3-phosphate dehydrogenase. (**H**) Flow cytometry plot (left) and analysis (right) of the frequency of IFN-γ^+ cells in *Stk40*$^{f/f}$ and *Stk40*$^{\Delta T}$ T_H1 cells transfected with control or *Foxo4* siRNA ($n = 3$ to 4). (**I**) Supernatants of differentiated *Stk40*$^{f/f}$ and *Stk40*$^{\Delta T}$ T_H1 cells transfected with control or *Foxo4* siRNA for 3 days were collected and the levels of IFN-γ were measured by ELISA ($n = 4$). Data are presented as means ± SD. *$P < 0.05$; ****$P < 0.0001$ (Student's *t* test). All data presented in this panel are the result of at least three independent experiments.

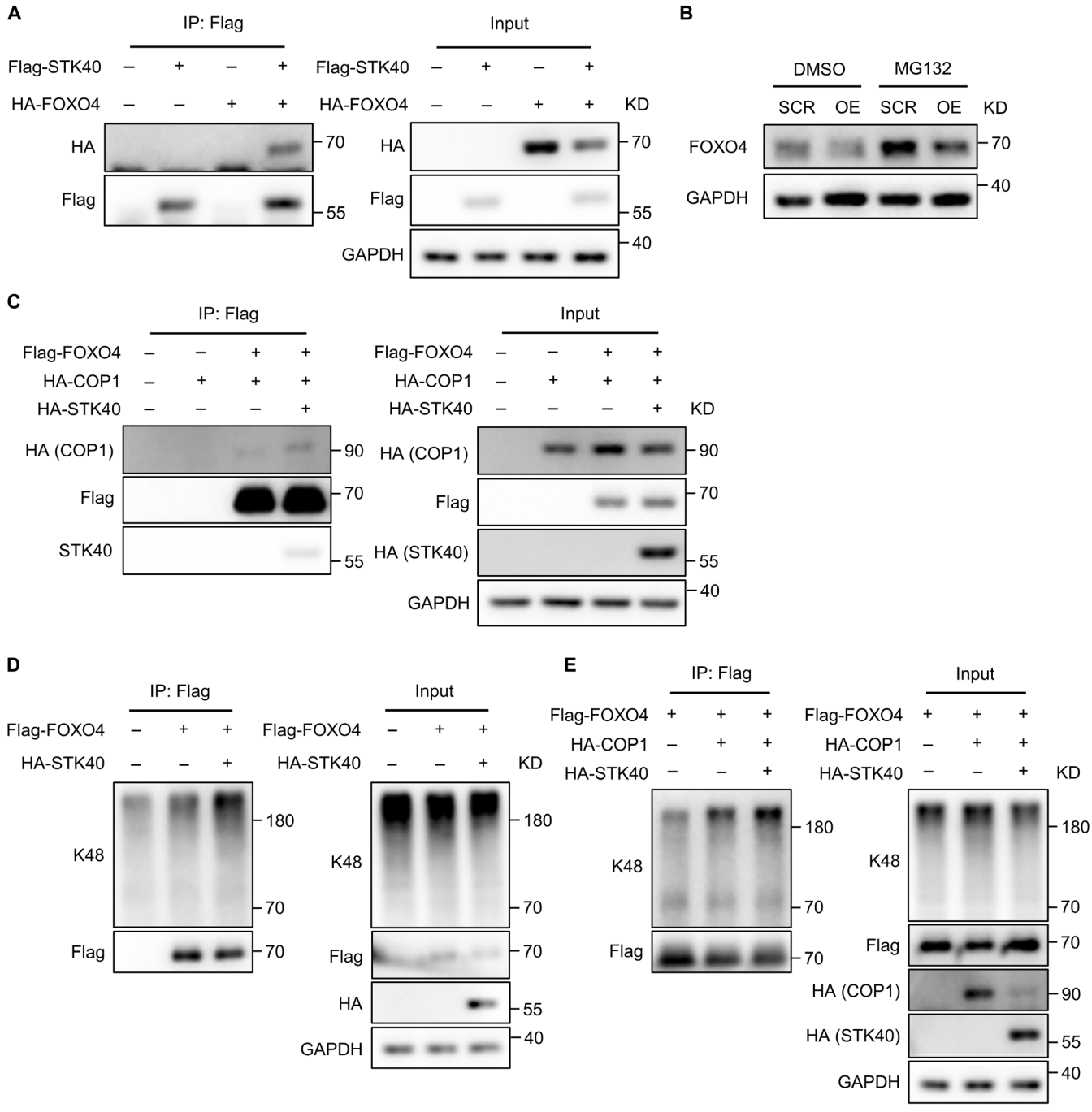

Fig. 8. STK40 promotes E3 ligase COP1-mediated K48-linked polyubiquitination of FOXO4. (**A**) Human embryonic kidney (HEK) 293T cells were transfected with HA-tagged FOXO4 along with or without Flag-tagged STK40. Cell lysates were immunoprecipitated with anti-Flag and analyzed by immunoblot. (**B**) SCR and OE Jurkat cells were treated with either 10 μM MG132 or dimethyl sulfoxide (DMSO) for 6 hours. Cells were collected and immunoblot analysis of FOXO4. (**C**) HEK293T cells were transfected with Flag-tagged FOXO4 and HA-tagged COP1 along with or without HA-tagged STK40. Cell lysates were immunoprecipitated with anti-Flag and analyzed by immunoblot. (**D**) Immunoblot analysis of K48-linked polyubiquitinated FOXO4 in HEK293T cells transfected with Flag-tagged FOXO4 along with or without HA-tagged STK40. (**E**) Immunoblot analysis of K48-conjugated ubiquitinated FOXO4 in HEK293T cells transfected with Flag-tagged FOXO4 and HA-tagged COP1 along with or without HA-tagged STK40. All data presented in this panel are the result of at least three independent experiments.

assumed that STK40 regulates T_H17 cell differentiation by targeting FOXO1. First, we detected an up-regulation of FOXO1 protein by immunoblotting in STK40-deficient naïve $CD4^+$ T cells cultured for 24 hours under T_H17-polarizing conditions (Fig. 9A). FOXO1 expression was also up-regulated in KD Jurkat cells, while FOXO1 expression was down-regulated in OE Jurkat cells compared to that in SCR Jurkat cells (Fig. 9B). Functioning as a transcription factor, FOXO1 enters nucleus; therefore, we separated the cytoplasm and nucleus of Jurkat cells and found that there was increased accumulation of FOXO1 in the nucleus of KD Jurkat cells, while the amount of FOXO1 in the nucleus of OE Jurkat cells was less than that of SCR Jurkat cells (fig. S6A). The above results demonstrate that STK40 negatively regulates FOXO1. Next, to demonstrate that STK40 promotes FOXO1 degradation through the proteasome pathway, we treated Jurkat cells with MG132 and found that FOXO1 protein was up-regulated in OE Jurkat cells after treatment (Fig. 9C). We then found that STK40 interacts with FOXO1 in HEK293T cells (Fig. 9D), and STK40 OE promotes K48-linked ubiquitination of the FOXO1 protein (Fig. 9E). Using co-IP assay, we found that the interaction between FOXO1 and COP1 was only detected when STK40 was overexpressed in HEK293T cells (Fig. 9F). Moreover, FOXO1 inhibitor AS1842856 treatment effectively promoted the differentiation of STK40-deficient T_H17 cells (Fig. 9G). These results suggest that STK40 down-regulates the expression of FOXO1 by mediating the binding of FOXO1 to COP1 and facilitating K48-linked ubiquitination of FOXO1, thereby promoting the differentiation of T_H17 cells.

In conclusion, our results demonstrate that STK40 functions as an adapter protein in the posttranslational regulation of FOXO1 and FOXO4 proteins (fig. S6B). Under conditions of T_H1 differentiation, STK40 promotes the interaction between FOXO4 and COP1, which enhances the K48-linked ubiquitination of FOXO4, leading to its degradation. As a result, IFN-γ expression is elevated in T_H1 cells. Likewise, STK40 facilitates the binding of FOXO1 and COP1 and promotes the K48-linked ubiquitination and degradation of FOXO1, thereby promoting the differentiation of T_H17 cells.

DISCUSSION

T_H1 and T_H17 cells are key factors driving the development of inflammation relative disease. However, the molecular mechanisms regulating T_H1 and T_H17 cell differentiation remain elusive. In this study, we identified the pseudokinase STK40 as a critical positive regulator of T_H1 and T_H17 differentiation. Deletion of STK40 impairs T_H1 and T_H17 cell differentiation in vitro as well as attenuates the severity of T_H1 and T_H17 cell–mediated pathological progression in EAE and DSS-induced acute colitis mouse models.

Pseudokinases play a crucial role in the regulation of a wide range of cellular processes and are known to be associated with key biological pathways that are frequently found to be dysregulated in many diseases. Despite the lack of typical phosphotransferase activity, pseudokinases play key roles as signaling mediators and protein scaffolds in normal and disease biology, often by promoting ubiquitination, facilitating the degradation of certain substrates, or modulating protein stability (*47*, *48*). STK40 acts as a scaffolding protein involved in E3 ligase COP1-mediated ubiquitination of substrates like c-Jun and C/EBPβ (*23*, *24*). Previous study showed that COP1 directly binds to FOXO4 and accelerates ubiquitination-mediated degradation of FOXO4 to promote tumorigenesis (*45*). In addition, Kato *et al.* (*46*) found that COP1 levels were induced by insulin in hepatocellular carcinoma cells and that COP1 binding to FOXO1 promoted the ubiquitin-dependent degradation of FOXO1. In current study, STK40 OE greatly enhanced the binding of COP1 to FOXO1/FOXO4 and the level of K48-linked polyubiquitination of FOXO1/FOXO4, and the inhibition of FOXO1/FOXO4 in T cells reversed the impairment of T_H1 or T_H17 cell differentiation caused by STK40 deficiency, demonstrating that STK40 functions as a scaffolding protein that assists COP1 in FOXO1/4 repression and thus facilitates T_H1 and T_H17 cell differentiation.

Dysregulation of T_H1 and T_H17 differentiation in vitro due to STK40 deletion is closely related to the milder EAE in $Stk40^{\Delta T}$ mice. Our study showed that STK40 deletion inhibited the in vitro differentiation of T_H1 and T_H17 cells, whereas the percentage of $IL\text{-}17A^+CD4^+$ cells in the CNS of EAE mice did not change significantly. Although past studies have shown that T_H17 is a key regulator mediating EAE disease development, it has been suggested that IL-17A is dispensable for EAE progression (*49*, *50*). Studies in recent years have shown that the presence of a population of GM-CSF-producing T helper (ThGM) cells during EAE plays a crucial role in disease development (*51*–*53*). A recent report indicated that pathogenic $IFN\text{-}\gamma^+GM\text{-}CSF^+$ T_H17 cells in EAE mice were derived from $IL\text{-}17A^+$ T_H17 cells in the intestine at steady state (*54*). Therefore, down-regulation of the proportion of $IFN\text{-}\gamma^+$ and $GM\text{-}CSF^+$ cells in the CNS of mice with EAE due to STK40 deletion here may indirectly reflect the dysregulation of differentiation of pathogenic T_H17 cells, while the exact mechanism needs to be further refined.

FOXO proteins are key molecules controlling T cell homeostasis and tolerance. A previous report clearly indicated that FOXO4 indirectly regulates IFN-γ production in T_H1 cells by targeting Dkk3 (*14*), while deletion of FOXO4 did not affect the expression of *Tbx21* and key factors associated with T_H1 identity. In our study, STK40 deletion resulted in the down-regulation of signature genes of T_H1 cells including *Tbx21*. KD of FOXO4 in STK40-deficient T_H1 cells was able to return *Ifng* expression to normal levels and partially rescued the down-regulation of *Tbx21* gene expression. IFN-γ is not only an effector cytokine produced by T_H1 but also a key cytokine that initiates downstream signaling cascade responses to form T_H1 cells (*55*). IFN-γ binds to the IFN-γ receptor on T cells via autocrine and induces the expression of the characteristic transcription factor T-bet in T_H1 cells by activating signaling through the STAT1 pathway (*4*). It cannot be excluded that the up-regulated expression of *Tbx21* in STK40-deficient T_H1 cells after inhibition of FOXO4 could be due to the increased production of IFN-γ, while the underlying mechanism needs to be further explored.

FOXO1 is recruited to a regulatory element located 22 kb upstream of the transcriptional start site of the *Ifng* gene in T_{reg} cells, and FOXO1-deficient T_{reg} cells produce large amounts of IFN-γ (*56*). Although it has been suggested that FOXO1 promotes the differentiation of T_H1 cells through directly promoting the transcription of the *Ifng* gene, there is evidence that the induction of T_H1 cells is greatly interrupted by treatment with AS1842856, an inhibitor of FOXO1 (*57*). We examined the expression of FOXO1, FOXO3a, and FOXO4 separately in STK40-deficient T_H1 cells and found that only FOXO4 was the most consistently up-regulated, while T_H17 differentiation was also inhibited in the absence of STK40. Past data showed that FOXO4 did not affect T_H17 differentiation. Then, we found that, in

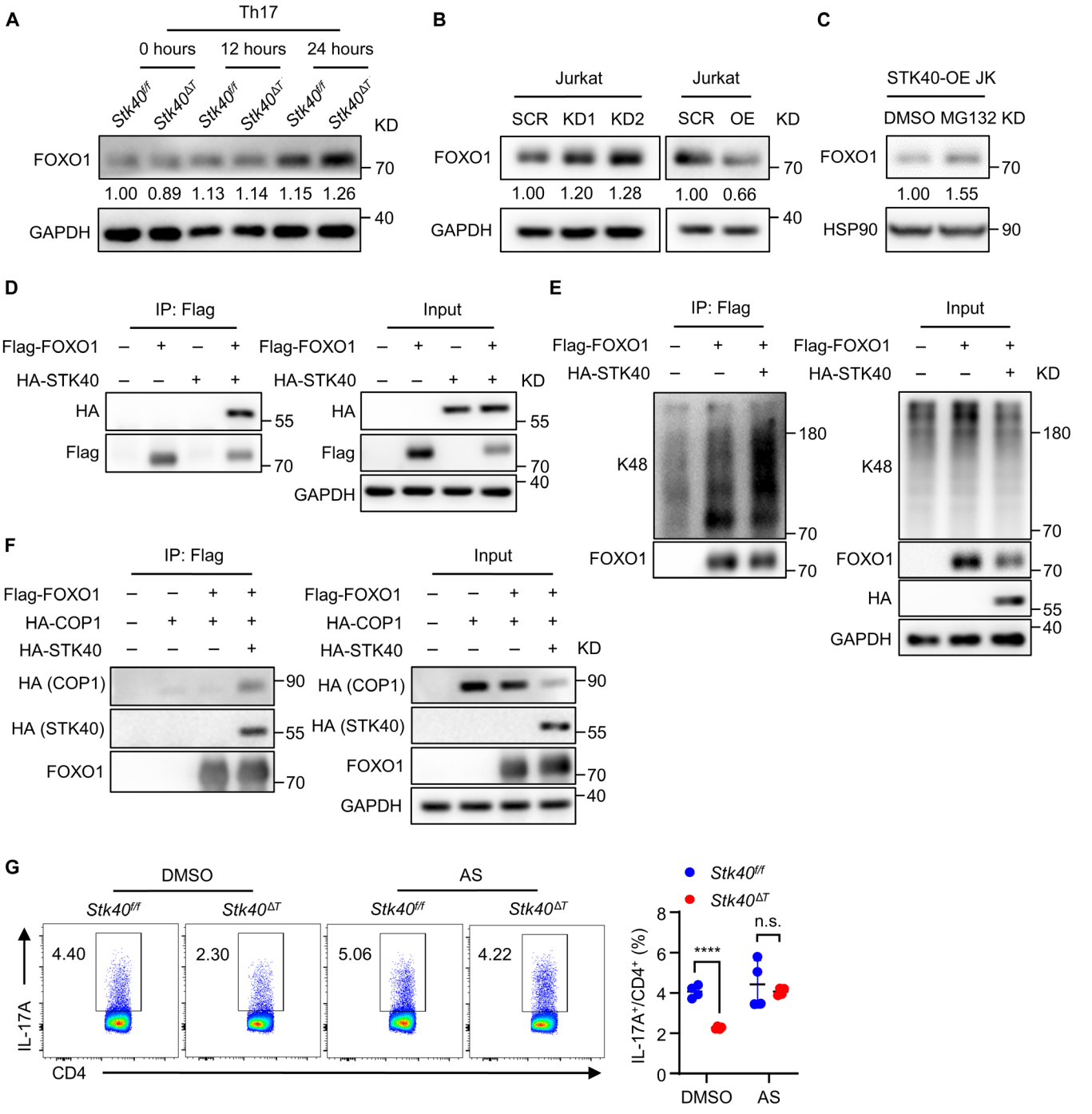

Fig. 9. STK40 up-regulates T_H17 cell differentiation through facilitating COP1-mediated K48-linked polyubiquitination of FOXO1. (**A**) Immunoblot analysis of the indicated proteins in *Stk40*$^{f/f}$ and *Stk40*$^{\Delta T}$ naïve CD4$^+$ T cells cultured under T_H17-polarizing conditions for indicated time. (**B**) Immunoblot analysis of the indicated proteins in SCR, KD, and OE Jurkat T cells. (**C**) OE Jurkat cells were treated with either 10 mM MG132 or DMSO for 6 hours. Cells were collected and immunoblot analysis of FOXO1. (**D**) HEK293T cells were transfected with Flag-tagged FOXO1 along with or without HA-tagged STK40. Cell lysates were immunoprecipitated with anti-Flag and analyzed by immunoblot. (**E**) Immunoblot analysis of K48-linked polyubiquitinated FOXO1 in HEK293T cells transfected with Flag-tagged FOXO1 along with or without HA-tagged STK40. (**F**) HEK293T cells were transfected with Flag-tagged FOXO1 and HA-tagged COP1 along with or without HA-tagged STK40. Cell lysates were immunoprecipitated with anti-Flag and analyzed by immunoblot. (**G**) Flow cytometry plot (left) and analysis (right) of the frequency of IL-17A$^+$ cells in *Stk40*$^{f/f}$ and *Stk40*$^{\Delta T}$ naïve CD4$^+$ T cells cultured under pT_H17-polarizing conditions in the presence of DMSO or AS1842856 (25 nM) ($n = 4$). Data are presented as means ± SD. ****$P < 0.0001$ (Student's t test). All data presented representative of at least three independent experiments. AS, AS1842856.

T_H17 cells, STK40 deletion led to up-regulation of FOXO1 protein. In addition, application of FOXO1 inhibitor effectively corrects the induction failure of T_H17 cells due to STK40 deficiency. Although we found that STK40 regulates FOXO1 and FOXO4 proteins by the same pathway, the details of STK40 regulation of FOXO4 and FOXO1, respectively, in T_H1 and T_H17 cells still need to be further understood.

Together, this study identifies a critical role for the pseudokinase STK40 in the differentiation of T_H1 and T_H17 cells. STK40 serves as a scaffolding protein that assists the E3 ligase COP1 and plays an important role in inflammatory and autoimmune diseases. Our findings provide a basis for further investigation of how pseudokinase family proteins regulate intracellular physiological functions and control the differentiation and function of $CD4^+$ T cells as well as other cells. Last, we assume that STK40 is a potential target for the therapy of autoimmune inflammatory diseases.

MATERIALS AND METHODS

Mice

Stk40$^{\Delta T}$ mice were obtained by crossing CD4-Cre mice (from the Jackson Laboratory) with *Stk40*$^{f/f}$ mice that were generated by GemPharmatech Co. Ltd. (China), using a LoxP targeting system. *Rag2*$^{-/-}$ mice were from Shanghai Model Organisms Center Inc. All mice were kept in a specific pathogen–free facility, and all mouse experiments were conducted following the protocols approved by the Institutional Animal Care and Use Committee of Shanghai Jiao Tong University School of Medicine (JUMC2023-028-A).

Cell lines

Jurkat T and HEK293T cell lines were purchased from American Type Culture Collection. The Jurkat T cells were cultured in RPMI 1640 medium supplemented with 10% fetal bovine serum (FBS) and 1% penicillin and streptomycin (Gibco). HEK293T cells were cultured in Dulbecco's modified Eagle's medium supplemented with 10% FBS, 2 mM L-glutamine (STEMCELL Technologies), and 1% penicillin and streptomycin.

T_H cell differentiation

Spleens were harvested from *Stk40*$^{f/f}$ or *Stk40*$^{\Delta T}$ mice. Mouse $CD4^+$ naïve T cells were isolated from splenocytes by magnetic negative selection using the EasySep Mouse Naïve $CD4^+$ T Cell Isolation Kit (STEMCELL Technologies). The $CD4^+$ naïve T cells were cultured in RPMI 1640 medium supplemented with 10% FBS, 1% penicillin and streptomycin, and plate-bound anti-CD3 (1 μg/ml) and anti-CD28 (1 μg/ml) with the following antibodies and cytokines for each T helper subset polarizing condition: T_H0: recombinant human IL-2 (rhIL-2; 30 U/ml) (PeproTech); T_H1: rhIL-2 (30 U/ml), recombinant mouse IL-12 (rmIL-12; 20 ng/ml) (PeproTech), and anti-IL-4 (1 μg/ml) (clone 11B11); T_H2: rhIL-2 (30 U/ml), rmIL-4 (12.5 ng/ml) (PeproTech), and anti–IFN-γ (1 μg/ml) (clone XMG1.2); iT_{reg}: rhIL-2 (30 U/ml), rhTGF-β1 (25 ng/ml) (PeproTech), and anti–IFN-γ (1 μg/ml); T_H17: rhTGF-β1 (2.5 ng/ml), rmIL-6 (20 ng/ml) (PeproTech), anti–IL-4 (1 μg/ml), and anti–IFN-γ (1 μg/ml); and pT_H17: rhTGF-β1 (2.5 ng/ml), rmIL-6 (20 ng/ml), rmIL-23 (20 ng/ml) (BioLegend), anti–IL-4 (1 μg/ml), and anti–IFN-γ (1 μg/ml).

DSS-induced colitis

DSS salt (M_w, 36,000 to 50,000 Da; Yeasen) was added to drinking water at a final concentration of 3% (w/v) and fed to 10- to 12-week-old mice for 7 days. The body weight of mice was monitored daily. On day 8, colons were collected for histological staining, and lamina propria cells were isolated for flow cytometry.

Adoptive transfer colitis

Naïve $CD4^+$ T cells ($CD4^+CD45RB^{hi}CD25^-$) were isolated from the spleen of 8-week-old female *Stk40*$^{f/f}$ and *Stk40*$^{\Delta T}$ mice using a BD FACSAria III cell sorter. A total of 5×10^5 naïve $CD4^+$ T cells were transferred into *Rag2*$^{-/-}$ mice, and recipient mice were measured body weight weekly.

EAE induction and activity

Ten- to 12-week-old mice were injected subcutaneously with 200 μg of MOG_{35-55} peptide [GL Biochem (Shanghai) Ltd.] in Freund's complete adjuvant containing heat-killed Mycobacterium tuberculosis H37Ra (5 mg/ml; BD Difco). On the day of immunization and 48 hours later, 200 ng of pertussis toxin (List Biological Laboratories) was administered intravenously. Clinical signs of EAE were assessed daily according to the following scores: 0, no clinical signs; 0.5, partially limp tail; 1, paralyzed tail; 2, loss in coordinated movement, hindlimb paresis; 2.5, one hindlimb paralyzed; 3, both hindlimbs paralyzed; 3.5, hindlimbs paralyzed, weakness in forelimbs; 4, forelimbs paralyzed; and 5, moribund or death. Data are reported as the mean daily clinical score. After the onset of EAE, food and water were provided on the cage floor.

Isolation of CNS leukocytes from EAE mice

For preparation of immune cells in the CNS, brain and spinal cord of MOG_{35-55}–immunized *Stk40*$^{f/f}$ and *Stk40*$^{\Delta T}$ mice were excised, grinded, and filtered through a 70-μm filter. Dispersed cells were layered onto a Percoll (GE Healthcare) density gradient and isolated by collection of the interface fraction between 37 and 70% Percoll. After intensive washing, the frequencies of immune cell subpopulations in the CNS were analyzed by flow cytometry.

Ex vivo recall responses

Splenocytes were harvested from mice at the day 10 of disease, counted, and cultured in 24-well microtiter plates at a density of 10^6 cells per well in a total volume of 0.5 ml of RPMI 1640 medium supplemented with 10% FBS and 1% penicillin and streptomycin. Cells were cultured at 37°C in the presence of MOG_{35-55} (20 μg/ml) or without any peptide for 72 hours.

T cell stimulation, proliferation, and ELISA

Mouse primary $CD4^+$ T cells and $CD8^+$ T cells were isolated from the spleen and peripheral lymph nodes of mice by the Mouse $CD4^+$ T Cell Isolation Kit and the PE Positive Selection Kit II (STEMCELL Technologies). Primary $CD4^+$ and $CD8^+$ T cells were stimulated with plate-bound anti-CD3 (1 μg/ml) and anti-CD28 (1 μg/ml) in replicate wells of 96-well plates (10^5 cells per well) for qPCR and immunoblot. T_H0, T_H1, and T_H17 cells were stimulated with plate-bound anti-CD3 (1 μg/ml) and anti-CD28 (1 μg/ml) in replicate wells of 24-well plates (10^6 cells per well) for ELISA, qPCR, and immunoblot assays. For T cell proliferation assay, isolated naïve $CD4^+$ T cells were labeled by Cell Proliferation Dye eFluor 450 (eBioscience), seeded in 96-well plates with three replicates under T_H1- and T_H17-polarized conditions for 3 days, and then were subjected to flow cytometry analyses. Serum or supernatants were collected, and the IL-2, IFN-γ, and IL-17A cytokine

level was measured by the ELISA Kit (Invitrogen) according to the manufacturers' instructions.

Histological analysis

The EAE mice were euthanized, and spinal cords that were dissected from mice transcardially perfused with 4% paraformaldehyde were fixed in 4% paraformaldehyde overnight, dehydrated with Ethanol and embedded in paraffin. Last, paraffin sections were counterstained with H&E or stained with Luxol fast blue.

Plasmid and transfections

HA-STK40–, Flag-STK40–, and HA-COP1–expressing plasmids were gifts from Y. Jin (Department of Histology, Embryology and Genetic Development, Shanghai Jiao Tong University School of Medicine, Shanghai, China). The HA-FOXO1–expressing plasmid was a gift from B. Liang (Center for Life Sciences, School of Life Sciences, Yunnan University, Kunming, Yunnan, China). The HA-FOXO4–expressing plasmid was a gift from M.-H. Lee (Sun Yat-sen University, Guangzhou, China). The Flag-FOXO4–expressing plasmid was a gift from P. Hu (Guangzhou Laboratory-Guangzhou Medical University, Guangzhou, China).

STK40 was cloned into pLVX-IRES-ZsGreen expression vector (Clontech, CA) to generate overexpressed human STK40 vector. shRNA of STK40 and shRNA control constructs described as previously were cloned into the pLKO.1 vector (Addgene). The sequences of STK40 shRNA are as follows: KD1: GCT CAT GAC TTC AGC GAT AAG; KD2: GCA GGA GCT CTT CCG CAA GAT. Lentivirus infection was used to knock down or overexpress STK40 in Jurkat T cells. Following procedures previously described in (*58*), one well of six-well plate containing 2×10^6 293T cells were transfected with 1.5 μg of plasmids, polyethylenimine (PEI), and packaging plasmids (psPAX2 and PMD.2G). After 48 hours, supernatants were collected, centrifuged, and filtered. Then, the virus-containing supernatant with polybrene (10 μg/ml; Sigma-Aldrich) was used to infect Jurkat T cell by centrifuging in 900*g* at 37°C for 1.5 hours. Stably transduced cells were enriched by puromycin selection or sorting green fluorescent protein–positive cells.

siRNA transfection

Mouse naïve $CD4^+$ T cells were cultured under T_H1-polarizing conditions without any penicillin/streptomycin. After 24 hours, *Foxo4* siRNA and negative control siRNA were mixed with LipoSmart 3000 Transfection Reagent (Getico) and then added to cells at 25 nM. After 16 hours, medium containing siRNAs was replaced with fresh medium containing T_H polarizing cytokines. Cells were incubated at 37°C for 3 days and then collected for further analysis. The sequences of *Foxo4* siRNA are as follows: sense: AGU CAU AUG CAG AAC UCA Utt; and antisense: AUG AGU UCU GCA UAU GAC Uga.

Western blot

The proteins were resolved by harvesting the cells after two washes and lysed on ice in radioimmunoprecipitation assay buffer for 15 min (20 mM tris-HCl, 2 mM EDTA, 1% NP-40, 10% glycerol, 150 mM NaCl, 1 mM phenylmethylsulfonyl fluoride, phosphatase inhibitors, and proteinase inhibitor cocktail). Cell lysates were centrifuged at 13,000 rpm and 4°C for 15 min, and protein concentration was determined. Then, protein was resolved by 10% SDS–polyacrylamide gel electrophoresis (SDS-PAGE) and electro-transferred onto polyvinylidene difluoride membrane (Immobilon-P). Membranes were blocked with 5% skim milk in 1× tris-buffered saline (TBS) buffer [50 mM tris-HCl (pH 7.5) and 150 mM NaCl] for 1 hour at room temperature and probed with each primary antibody overnight at 4°C. After twice washes with 1× TBS supplemented with 0.05% Tween 20, membranes were incubated with horseradish peroxidase (HRP)–conjugated secondary antibody (Cell Signaling Technology) and then detected by enhanced chemiluminescence detection (Tanon). All primary antibodies were used at a 1:1000 dilution, with secondary HRP antibodies used at 1:5000 (diluted in 5% skim milk) (*58*).

Immunoprecipitation

To detect K48-linked polyubiquitination of exogenous protein in 293T cells, cells were lysed in NP-40 lysis buffer [50 mM tris (pH 7.6), 150 mM NaCl, and 1% v/v NP-40] with 10 mM *N*-ethylmaleimide (Sigma-Aldrich) and complete protease inhibitor mixture (Roche Diagnostic). Samples were incubated at 4°C for 30 min, followed by centrifugation at 13,000*g* for 10 min at 4°C. The supernatants were immunoprecipitated with anti-FLAG M2 Affinity Gel (Selleck) for 12 hours at 4°C. The immunoprecipitants were washed three times with NP-40 buffer. An aliquot (50 μl) of 1× SDS-loading buffer was added to the beads. Samples were resolved SDS-PAGE for immunoblot analysis.

For co-IP assay, cells were lysed in NP-40 lysis buffer with complete protease inhibitor mixture. Samples were incubated at 4°C for 30 min, followed by centrifugation at 13,000*g* for 10 min at 4°C. The supernatants were immunoprecipitated with anti-FLAG M2 Affinity Gel for 12 hours at 4°C. The immunoprecipitants were washed three times with NP-40 buffer and boiled in 1× SDS-loading buffer for immunoblot analysis.

Flow cytometry

A single-cell suspension was prepared from thymus, spleen, lymph nodes, CNS, or colon. Live cells were selected after staining with Fixable Viability Stain (BD Biosciences). For analysis of surface markers, cells were blocked by α-CD16/32 antibody (1:200) and stained by primary antibody (1:200) in fluorescence-activated cell sorting buffer (phosphate-buffered saline, 2% FBS, and 2 mM EDTA) at 4°C for 30 min. To detect intracellular cytokine production, cells were stimulated with stimulation cocktail (Invitrogen) for 12 to 16 hours before fixation and permeabilization using the Cytofix/Cytoperm Fixation/Permeabilization Kit (BD Biosciences), according to the manufacturer's instructions, and subjected to antibody staining (1:100). For transcription factor staining, surface marker-stained cells were fixed, permeabilized using an eBioscience Transcription Factor Fixation/Permeabilization staining kit (Invitrogen), and labeled with specific transcription factor antibodies (1:100). Flow cytometry data were acquired on FACSVerse or LSR Fortessa (BD Biosciences) and analyzed with FlowJo_VX software (Tree Star) (*58*).

Quantification and statistical analysis

All the experiments were independently repeated at least three times. The exact values of *n* are specified in the respective figure legends. Data are expressed as means ± SD. Statistical analysis was performed with GraphPad PRISM software 8.0.2 (GraphPad Inc., La Jolla, CA, USA). Significances are indicated with $^*P \leq 0.05$, $^{**}P \leq 0.01$, and $^{***}P \leq 0.001$, and $^{****}P \leq 0.0001$.

Supplementary Materials

This PDF file includes:

Supplementary Materials and Methods
Figs. S1 to S6

REFERENCES AND NOTES

1. L. Zhou, M. M. Chong, D. R. Littman, Plasticity of $CD4^+$ T cell lineage differentiation. *Immunity* **30**, 646–655 (2009).
2. T. Korn, E. Bettelli, M. Oukka, V. K. Kuchroo, IL-17 and Th17 Cells. *Annu. Rev. Immunol.* **27**, 485–517 (2009).
3. M. Afkarian, J. R. Sedy, J. Yang, N. G. Jacobson, N. Cereb, S. Y. Yang, T. L. Murphy, K. M. Murphy, T-bet is a STAT1-induced regulator of IL-12R expression in naïve $CD4^+$ T cells. *Nat. Immunol.* **3**, 549–557 (2002).
4. S. J. Szabo, S. T. Kim, G. L. Costa, X. Zhang, C. G. Fathman, L. H. Glimcher, A novel transcription factor, T-bet, directs Th1 lineage commitment. *Cell* **100**, 655–669 (2000).
5. W. E. Thierfelder, J. M. van Deursen, K. Yamamoto, R. A. Tripp, S. R. Sarawar, R. T. Carson, M. Y. Sangster, D. A. Vignali, P. C. Doherty, G. C. Grosveld, J. N. Ihle, Requirement for Stat4 in interleukin-12-mediated responses of natural killer and T cells. *Nature* **382**, 171–174 (1996).
6. M. Sospedra, R. Martin, Immunology of multiple sclerosis. *Annu. Rev. Immunol.* **23**, 683–747 (2005).
7. A. Geremia, P. Biancheri, P. Allan, G. R. Corazza, A. Di Sabatino, Innate and adaptive immunity in inflammatory bowel disease. *Autoimmun. Rev.* **13**, 3–10 (2014).
8. P. R. Mangan, L. E. Harrington, D. B. O'Quinn, W. S. Helms, D. C. Bullard, C. O. Elson, R. D. Hatton, S. M. Wahl, T. R. Schoeb, C. T. Weaver, Transforming growth factor-β induces development of the T_H17 lineage. *Nature* **441**, 231–234 (2006).
9. I. I. Ivanov, B. S. McKenzie, L. Zhou, C. E. Tadokoro, A. Lepelley, J. J. Lafaille, D. J. Cua, D. R. Littman, The orphan nuclear receptor RORγ directs the differentiation program of proinflammatory IL-17^+ T helper cells. *Cell* **126**, 1121–1133 (2006).
10. M. J. McGeachy, K. S. Bak-Jensen, Y. Chen, C. M. Tato, W. Blumenschein, T. McClanahan, D. J. Cua, TGF-β and IL-6 drive the production of IL-17 and IL-10 by T cells and restrain T_H-17 cell-mediated pathology. *Nat. Immunol.* **8**, 1390–1397 (2007).
11. M. J. McGeachy, Y. Chen, C. M. Tato, A. Laurence, B. Joyce-Shaikh, W. M. Blumenschein, T. K. McClanahan, J. J. O'Shea, D. J. Cua, The interleukin 23 receptor is essential for the terminal differentiation of interleukin 17-producing effector T helper cells in vivo. *Nat. Immunol.* **10**, 314–324 (2009).
12. C. Wu, N. Yosef, T. Thalhamer, C. Zhu, S. Xiao, Y. Kishi, A. Regev, V. K. Kuchroo, Induction of pathogenic T_H17 cells by inducible salt-sensing kinase SGK1. *Nature* **496**, 513–517 (2013).
13. C. Stienne, M. F. Michieletto, M. Benamar, N. Carrié, I. Bernard, X. H. Nguyen, Y. Lippi, F. Duguet, R. S. Liblau, S. M. Hedrick, A. Saoudi, A. S. Dejean, Foxo3 transcription factor drives pathogenic T helper 1 differentiation by inducing the expression of Eomes. *Immunity* **45**, 774–787 (2016).
14. X. Chen, J. Hu, Y. Wang, Y. Lee, X. Zhao, H. Lu, G. Zhu, H. Wang, Y. Jiang, F. Liu, Y. Chen, B. S. Kim, Q. Zhou, X. Liu, X. Wang, S. H. Chang, C. Dong, The FoxO4/DKK3 axis represses IFN-γ expression by Th1 cells and limits antimicrobial immunity. *J. Clin. Invest.* **132**, e147566 (2022).
15. H. Huang, D. J. Tindall, Regulation of FOXO protein stability via ubiquitination and proteasome degradation. *Biochim. Biophys. Acta* **1813**, 1961–1964 (2011).
16. J. Huang, L. Teng, T. Liu, L. Li, D. Chen, F. Li, L. G. Xu, Z. Zhai, H. B. Shu, Identification of a novel serine/threonine kinase that inhibits TNF-induced NF-κB activation and p53-induced transcription. *Biochem. Biophys. Res. Commun.* **309**, 774–778 (2003).
17. I. Durzynska, X. Xu, G. Adelmant, S. B. Ficarro, J. A. Marto, P. Sliz, S. Uljon, S. C. Blacklow, STK40 is a pseudokinase that binds the E3 ubiquitin ligase COP1. *Structure* **25**, 287–294 (2017).
18. J. E. Kung, N. Jura, Prospects for pharmacological targeting of pseudokinases. *Nat. Rev. Drug Discov.* **18**, 501–526 (2019).
19. J. E. Kung, N. Jura, Structural basis for the non-catalytic functions of protein kinases. *Structure* **24**, 7–24 (2016).
20. L. Li, L. Sun, F. Gao, J. Jiang, Y. Yang, C. Li, J. Gu, Z. Wei, A. Yang, R. Lu, Y. Ma, F. Tang, S. W. Kwon, Y. Zhao, J. Li, Y. Jin, Stk40 links the pluripotency factor Oct4 to the Erk/MAPK pathway and controls extraembryonic endoderm differentiation. *Proc. Natl. Acad. Sci. U.S.A.* **107**, 1402–1407 (2010).
21. H. Yu, K. He, L. Wang, J. Hu, J. Gu, C. Zhou, R. Lu, Y. Jin, Stk40 represses adipogenesis through translational control of CCAAT/enhancer-binding proteins. *J. Cell Sci.* **128**, 2881–2890 (2015).
22. H. Yu, K. He, L. Li, L. Sun, F. Tang, R. Li, W. Ning, Y. Jin, Deletion of STK40 protein in mice causes respiratory failure and death at birth. *J. Biol. Chem.* **288**, 5342–5352 (2013).
23. J. Hu, S. Li, X. Sun, Z. Fang, L. Wang, F. Xiao, M. Shao, L. Ge, F. Tang, J. Gu, H. Yu, Y. Guo, X. Guo, B. Liao, Y. Jin, *Stk40* deletion elevates c-JUN protein level and impairs mesoderm differentiation. *J. Biol. Chem.* **294**, 9959–9972 (2019).
24. A. Ndoja, R. Reja, S. H. Lee, J. D. Webster, H. Ngu, C. M. Rose, D. S. Kirkpatrick, Z. Modrusan, Y. J. Chen, D. L. Dugger, V. Gandham, L. Xie, K. Newton, V. M. Dixit, Ubiquitin ligase COP1 suppresses neuroinflammation by degrading c/EBPβ in microglia. *Cell* **182**, 1156–1169. e12 (2020).
25. P. A. Eyers, K. Keeshan, N. Kannan, Tribbles in the 21st century: The evolving roles of Tribbles pseudokinases in biology and disease. *Trends Cell Biol.* **27**, 284–298 (2017).
26. K. Keeshan, Y. He, B. J. Wouters, O. Shestova, L. Xu, H. Sai, C. G. Rodriguez, I. Maillard, J. W. Tobias, P. Valk, M. Carroll, J. C. Aster, R. Delwel, W. S. Pear, Tribbles homolog 2 inactivates C/EBPα and causes acute myelogenous leukemia. *Cancer Cell* **10**, 401–411 (2006).
27. T. Yokoyama, Y. Kanno, Y. Yamazaki, T. Takahara, S. Miyata, T. Nakamura, Trib1 links the MEK1/ERK pathway in myeloid leukemogenesis. *Blood* **116**, 2768–2775 (2010).
28. R. Hill, P. A. Madureira, B. Ferreira, I. Baptista, S. Machado, L. Colaço, M. Dos Santos, N. Liu, A. Dopazo, S. Ugurel, A. Adrienn, E. Kiss-Toth, M. Isbilen, A. O. Gure, W. Link, TRIB2 confers resistance to anti-cancer therapy by activating the serine/threonine protein kinase AKT. *Nat. Commun.* **8**, 14687 (2017).
29. N. Zareen, S. C. Biswas, L. A. Greene, A feed-forward loop involving Trib3, Akt and FoxO mediates death of NGF-deprived neurons. *Cell Death Differ.* **20**, 1719–1730 (2013).
30. K. S. Rome, S. J. Stein, M. Kurachi, J. Petrovic, G. W. Schwartz, E. A. Mack, S. Uljon, W. W. Wu, A. G. DeHart, S. E. McClory, L. Xu, P. A. Gimotty, S. C. Blacklow, R. B. Faryabi, E. J. Wherry, M. S. Jordan, W. S. Pear, Trib1 regulates T cell differentiation during chronic infection by restraining the effector program. *J. Exp. Med.* **217**, e20190888 (2020).
31. C. Miyajima, Y. Itoh, Y. Inoue, H. Hayashi, Positive regulation of interleukin-2 expression by a pseudokinase, Tribbles 1, in activated T cells. *Biol. Pharm. Bull.* **38**, 1126–1133 (2015).
32. E. Dugast, E. Kiss-Toth, L. Docherty, R. Danger, M. Chesneau, V. Pichard, J. P. Judor, S. Pettré, S. Conchon, J. P. Soulillou, S. Brouard, J. Ashton-Chess, Identification of tribbles-1 as a novel binding partner of Foxp3 in regulatory T cells. *J. Biol. Chem.* **288**, 10051–10060 (2013).
33. K. L. Liang, C. O'Connor, J. P. Veiga, T. V. McCarthy, K. Keeshan, TRIB2 regulates normal and stress-induced thymocyte proliferation. *Cell Discov.* **2**, 15050 (2016).
34. P. M. Smith, W. S. Garrett, The gut microbiota and mucosal T cells. *Front. Microbiol.* **2**, 111 (2011).
35. M. F. Neurath, Cytokines in inflammatory bowel disease. *Nat. Rev. Immunol.* **14**, 329–342 (2014).
36. P. Jiang, C. Zheng, Y. Xiang, S. Malik, D. Su, G. Xu, M. Zhang, The involvement of TH17 cells in the pathogenesis of IBD. *Cytokine Growth Factor Rev.* **69**, 28–42 (2023).
37. J. T. Chang, Pathophysiology of inflammatory bowel diseases. *N. Engl. J. Med.* **383**, 2652–2664 (2020).
38. J. Oh, A. Vidal-Jordana, X. Montalban, Multiple sclerosis: Clinical aspects. *Curr. Opin. Neurol.* **31**, 752–759 (2018).
39. C. S. Constantinescu, N. Farooqi, K. O'Brien, B. Gran, Experimental autoimmune encephalomyelitis (EAE) as a model for multiple sclerosis (MS). *Br. J. Pharmacol.* **164**, 1079–1106 (2011).
40. A. Jain, R. A. Irizarry-Caro, M. M. McDaniel, A. S. Chawla, K. R. Carroll, G. R. Overcast, N. H. Philip, A. Oberst, A. V. Chervonsky, J. D. Katz, C. Pasare, T cells instruct myeloid cells to produce inflammasome-independent IL-1β and cause autoimmunity. *Nat. Immunol.* **21**, 65–74 (2020).
41. V. Kandula, R. Kosuru, H. Li, D. Yan, Q. Zhu, Q. Lian, R. S. Ge, Z. Xia, M. G. Irwin, Forkhead box transcription factor 1: Role in the pathogenesis of diabetic cardiomyopathy. *Cardiovasc. Diabetol.* **15**, 44 (2016).
42. A. Eijkelenboom, B. M. Burgering, FOXOs: Signalling integrators for homeostasis maintenance. *Nat. Rev. Mol. Cell Biol.* **14**, 83–97 (2013).
43. Y. M. Kerdiles, E. L. Stone, D. R. Beisner, M. A. McGargill, I. L. Ch'en, C. Stockmann, C. D. Katayama, S. M. Hedrick, Foxo transcription factors control regulatory T cell development and function. *Immunity* **33**, 890–904 (2010).
44. W. Ouyang, O. Beckett, Q. Ma, J. H. Paik, R. A. DePinho, M. O. Li, Foxo proteins cooperatively control the differentiation of $Foxp3^+$ regulatory T cells. *Nat. Immunol.* **11**, 618–627 (2010).
45. H. H. Choi, S. Zou, J. L. Wu, H. Wang, L. Phan, K. Li, P. Zhang, D. Chen, Q. Liu, B. Qin, T. A. T. Nguyen, S. J. Yeung, L. Fang, M. H. Lee, EGF relays signals to COP1 and facilitates FOXO4 degradation to promote tumorigenesis. *Adv. Sci.* **7**, 2000681 (2020).
46. S. Kato, J. Ding, E. Pisck, U. S. Jhala, K. Du, COP1 functions as a FoxO1 ubiquitin E3 ligase to regulate FoxO1-mediated gene expression. *J. Biol. Chem.* **283**, 35464–35473 (2008).
47. J. M. Murphy, Y. Nakatani, S. A. Jamieson, W. Dai, I. S. Lucet, P. D. Mace, Molecular mechanism of CCAAT-enhancer binding protein recruitment by the TRIB1 pseudokinase. *Structure* **23**, 2111–2121 (2015).
48. K. Li, F. Wang, W. B. Cao, X. X. Lv, F. Hua, B. Cui, J. J. Yu, X. W. Zhang, S. Shang, S. S. Liu, J. M. Yu, M. Z. Han, B. Huang, T. T. Zhang, X. Li, J. D. Jiang, Z. W. Hu, TRIB3 promotes APL progression through stabilization of the oncoprotein PML-RARα and inhibition of p53-mediated senescence. *Cancer Cell* **31**, 697–710.e7 (2017).
49. S. Haak, A. L. Croxford, K. Kreymborg, F. L. Heppner, S. Pouly, B. Becher, A. Waisman, IL-17A and IL-17F do not contribute vitally to autoimmune neuro-inflammation in mice. *J. Clin. Invest.* **119**, 61–69 (2009).

50. A. M. McGinley, C. E. Sutton, S. C. Edwards, C. M. Leane, J. DeCourcey, A. Teijeiro, J. A. Hamilton, L. Boon, N. Djouder, K. H. G. Mills, Interleukin-17 a serves a priming role in autoimmunity by recruiting IL-1β-producing myeloid cells that promote pathogenic T cells. *Immunity* **52**, 342–356.e6 (2020).
51. J. Komuczki, S. Tuzlak, E. Friebel, T. Hartwig, S. Spath, P. Rosenstiel, A. Waisman, L. Opitz, M. Oukka, B. Schreiner, P. Pelczar, B. Becher, Fate-mapping of GM-CSF expression identifies a discrete subset of inflammation-driving T helper cells regulated by cytokines IL-23 and IL-1β. *Immunity* **50**, 1289–1304.e6 (2019).
52. J. Rasouli, G. Casella, S. Yoshimura, W. Zhang, D. Xiao, J. Garifallou, M. V. Gonzalez, A. Wiedeman, A. Kus, E. R. Mari, P. Fortina, H. Hakonarson, S. A. Long, G. X. Zhang, B. Ciric, A. Rostami, A distinct GM-CSF$^+$ T helper cell subset requires T-bet to adopt a T_H1 phenotype and promote neuroinflammation. *Sci. Immunol.* **5**, eaba9953 (2020).
53. E. Galli, F. J. Hartmann, B. Schreiner, F. Ingelfinger, E. Arvaniti, M. Diebold, D. Mrdjen, F. van der Meer, C. Krieg, F. A. Nimer, N. Sanderson, C. Stadelmann, M. Khademi, F. Piehl, M. Claassen, T. Derfuss, T. Olsson, B. Becher, GM-CSF and CXCR4 define a T helper cell signature in multiple sclerosis. *Nat. Med.* **25**, 1290–1300 (2019).
54. A. Schnell, L. Huang, M. Singer, A. Singaraju, R. M. Barilla, B. M. L. Regan, A. Bollhagen, P. I. Thakore, D. Dionne, T. M. Delorey, M. Pawlak, G. M. Zu Horste, O. Rozenblatt-Rosen, R. A. Irizarry, A. Regev, V. K. Kuchroo, Stem-like intestinal Th17 cells give rise to pathogenic effector T cells during autoimmunity. *Cell* **184**, 6281–6298.e23 (2021).
55. A. A. Lighvani, D. M. Frucht, D. Jankovic, H. Yamane, J. Aliberti, B. D. Hissong, B. V. Nguyen, M. Gadina, A. Sher, W. E. Paul, J. J. O'Shea, T-bet is rapidly induced by interferon-γ in lymphoid and myeloid cells. *Proc. Natl. Acad. Sci. U.S.A.* **98**, 15137–15142 (2001).
56. W. Ouyang, W. Liao, C. T. Luo, N. Yin, M. Huse, M. V. Kim, M. Peng, P. Chan, Q. Ma, Y. Mo, D. Meijer, K. Zhao, A. Y. Rudensky, G. Atwal, M. Q. Zhang, M. O. Li, Novel Foxo1-dependent transcriptional programs control T_{reg} cell function. *Nature* **491**, 554–559 (2012).
57. E. E. Kraus, L. Kakuk-Atkins, M. F. Farinas, M. Jeffers, A. E. Lovett-Racke, Y. Yang, Regulation of autoreactive CD4 T cells by FoxO1 signaling in CNS autoimmunity. *J. Neuroimmunol.* **359**, 577675 (2021).
58. H. Xiang, Y. Tao, Z. Jiang, X. Huang, H. Wang, W. Cao, J. Li, R. Ding, M. Shen, R. Feng, L. Li, C. Guan, J. Liu, J. Ni, L. Chen, Z. Wang, Y. Ye, Q. Zhong, J. Liu, Q. Zou, X. Wu, Vps33B controls Treg cell suppressive function through inhibiting lysosomal nutrient sensing complex-mediated mTORC1 activation. *Cell Rep.* **39**, 110943 (2022).

Acknowledgments: We thank Y. Jin (Shanghai Jiao Tong University School of Medicine) for providing *Stk40$^{f/f}$* mice. **Funding:** This work was supported by the National Key Research and Development Program of China (grant 2021YFC2701800), National Natural Science Foundation of China (grants 31670910 and 82170748), Science and Technology Innovation Plan of Shanghai Science and Technology Commission (grants 21ZR1456200 and 23ZR1455400), Innovative Research Team of High-Level Local Universities in Shanghai (grant SHSMUZDCX20212000), and Shanghai Frontiers Science Center of Cellular Homeostasis Regulation and Human Diseases. **Author contributions:** Conceptualization: Y.T., H.X., T.Z., B.L., and X.W. Methodology: Y.T., J. Li, J.H., H.W., X.L., H.X., Z.J., J.N., C.G., J. Liu, Y.J., T.Z., B.L., and X.W. Investigation: Y.T., H.W., Z.J., J.N., and T.Z. Validation: Y.T., J. Li, W.C., H.W., T.Z., and X.W. Resources: H.X., K.H., L.W., Y.J., B.L., T.Z., and X.W. Formal analysis: Y.T., D.L., and T.Z. Visualization: T.Z. and X.W. Data curation: H.W. and T.Z. Funding acquisition: J.N., T.Z., and X.W. Supervision: H.W., H.X., T.Z., and X.W. Project administration: Y.T., H.W., T.Z., and X.W. Software: T.Z. Writing—original draft: Y.T. and T.Z. Writing—review and editing: Y.T., H.W., H.X., J.N., J. Liu, L.W., B.L., T.Z., and X.W. **Competing interests:** The authors declare that they have no competing interests. **Data and materials availability:** All data needed to evaluate the conclusions in the paper are present in the paper and/or the Supplementary Materials. RNA-seq data are provided via the Sequence Read Archive (SRA), accession number PRJNA1136166.

Submitted 18 March 2024
Accepted 18 October 2024
Published 20 November 2024
10.1126/sciadv.adp2919